0031-6997/98/5003-0387$03.00/0
PHARMACOLOGICAL REVIEWS
Vol. 50, No. 3

*Printed in U.S.A.*



# Prediction of Pharmacokinetic Alterations Caused by Drug-Drug Interactions: Metabolic Interaction in the Liver

K. ITO, T. IWATSUBO, S. KANAMITSU, K. UEDA, H. SUZUKI, AND Y. SUGIYAMA[a]

*Department of Pharmaceutics, Faculty of Pharmaceutical Sciences, University of Tokyo, 7-3-1 Hongo, Bunkyo-ku, Tokyo 113-0033, Japan.*

This paper is available online at http://www.pharmrev.org



## I. Introduction

Serious side-effects caused by drug interactions have attracted a great deal of attention and have become a social problem since the coadministration of ketoconazole and terfenadine was reported to cause potentially life-threatening ventricular arrhythmias (Monahan *et al.,* 1990), and an interaction between sorivudine and fluorouracil resulted in fatal toxicity in Japan (Watabe, 1996; Okuda *et al.,* 1997). The possible sites of drug-drug interaction which can change pharmacokinetic profiles include: (1) gastrointestinal absorption, (2) plasma and/or tissue protein binding, (3) carrier-mediated transport across plasma membranes (including hepatic or renal uptake and biliary or

[a] Address for correspondence: Yuichi Sugiyama, Department of Pharmaceutics, Faculty of Pharmaceutical Sciences, University of Tokyo, 7-3-1 Hongo, Bunkyo-ku, Tokyo 113-0033, Japan, Phone: 81-3-5689-8094, Fax: 81-3-5800-6949, E-mail: sugiyama@seizai.f.u-tokyo.ac.jp.

urinary secretion), and (4) metabolism. Pharmacodynamic interactions such as antagonism at the receptor may also increase or decrease the effects of a drug.

In this review, after brief comments on (2) and (3), we intend to focus on (4) and to discuss the possibility of the quantitative prediction of drug-drug interactions in vivo based on the analyses of data from literature obtained by in vitro experiments using human liver samples. Furthermore, strategic proposals for avoiding toxic interactions will be given from a pharmacokinetic point of view.

## II. Drug-Drug Interactions Other Than Involving Metabolism

### *A. Drug-drug interactions involving plasma protein binding*

Although interactions involving plasma protein binding are well known, they rarely cause clinically serious problems (Rowland and Tozer, 1995; Rolan, 1994). The reasons are summarized below.

The unbound fraction ($f_u$)[b] of a drug in plasma is increased when it is displaced by other drugs at the plasma protein binding sites. Subsequent alterations in plasma concentration profiles can be caused by changes in both clearance (CL) and volume of distribution ($V_d$) of the drug. The effect on the steady-state concentration ($C_{ss}$) and the area under concentration-time curve (AUC) can be predicted from the change in CL. It should be noted that the effect of protein binding replacement depends on the magnitude of CL and the route of administration. As shown in table 1, an analysis based on the well-stirred model has revealed that the protein binding replacement has little effect on the $C_{ss}$ and AUC for unbound drugs ($C_{u,ss}$ and $AUC_u$) after oral administration, which are parameters directly related to the pharmacological and adverse effects, irrespective of the magnitude of CL. In the case of low clearance drugs, $C_{u,ss}$ and $AUC_u$ after intravenous administration also are affected little by protein binding replacement. The only situation for a possible interaction is after the intravenous administration of a high clearance drug and there are few examples of this in clinical practice (Rolan, 1994).

The alteration of $V_d$ caused by protein binding replacement also has an effect on the blood drug concentration (Rowland and Tozer, 1995). In the case of drugs with a relatively large $V_d$, $V_d$ increases in parallel with $f_u$. Although this leads to a transient reduction in total

TABLE 1

*Relationship between the area under concentration-time curve (AUC) or AUC for unbound drugs ($AUC_u$) and the hepatic blood flow ($Q_h$), the hepatic intrinsic clearance ($CL_{int,h}$), and the blood unbound fraction ($f_b$) based on the well-stirred model (Wilkinson, 1983)*

| Administration | Condition | $AUC_{total}$ | $AUC_u$ |
|---|---|---|---|
| | General | $\frac{D(Q_h + f_b \cdot CL_{int,h})}{Q_h \cdot f_b \cdot CL_{int,h}}$ | $\frac{D(Q_h + f_b \cdot CL_{int,h})}{Q_h \cdot CL_{int,h}}$ |
| Intravenous | $Q_h \ll f_b \cdot CL_{int,h}$ | $\frac{D}{Q_h}$ | $\frac{D \cdot f_b}{Q_h}$ |
| | $Q_h \gg f_b \cdot CL_{int,h}$ | $\frac{D}{f_b \cdot CL_{int,h}}$ | $\frac{D}{CL_{int,h}}$ |
| Oral | All | $\frac{D}{f_b \cdot CL_{int,h}}$ | $\frac{D}{CL_{int,h}}$ |

[b] Abbreviations: $\alpha_1$, membrane permeation constant from the lumen into the cell; 5,FU, 5-fluorouracil; ATP, adenosine triphosphate; AUC, area under concentration-time curve; $AUC_{IV}$, AUC after intravenous administration; $AUC_{po}$, AUC after oral administration; $AUC_u$, AUC for unbound drugs; BA, bioavailability; BBM, brush border membrane; BLM, basolateral membrane; BVU, 5-bromovinyluracil; C/M ratio, cell-to-medium unbound concentration ratio; $C_{cell}$, steady-state total drug concentration in the cell; $C_{cell,free}$, steady-state unbound drug concentration in the cell; $C_h$, concentration in the liver; CL, clearance; $CL_h$, hepatic clearance; $CL_{h,m}$, clearance for a particular metabolic pathway; $CL_{int}$, intrinsic clearance for metabolism; $CL_{int,all}$, overall intrinsic clearance; $CL_{oral}$, oral clearance; $CL_r$, renal clearance; $CL_{tot}$, total clearance; $C_{max}$, maximum concentration; $C_{medium}$, steady-state total drug concentration in the medium; $C_{portal}$, concentration in portal vein; $C_{ss}$, steady-state concentration; $C_{sys}$, concentration in systemic blood; $C_{u,ss}$, $C_{ss}$ for unbound drugs; D, dose; DBSP, dibromosulfophthalein; DPD, dihydropyrimidine dehydrogenase; E, enzyme; $E_{act}$, amount of active enzyme; $E_g$, gut extraction ratio; $E_h$, hepatic extraction ratio; EI, enzyme-inhibitor complex; $E_{inact}$, amount of inactive enzyme; EIS, enzyme-inhibitor-substrate complex; $E_o$, total concentration of the enzyme; ES, enzyme-substrate complex; $F_a$, fraction of drug absorbed from the gastrointestinal tract into the portal vein; $F_{abs}$, fraction of drug dose absorbed into and through the gastrointestinal membranes; $f_b$, unbound fraction in blood; $F_g$, fraction of absorbed dose that passes through the gut into the hepatic portal blood unmetabolized; $f_h$, fraction of $CL_h$ in $CL_{tot}$; $F_h$, hepatic availability; $f_m$, fraction of the metabolic process subject to inhibition in $CL_h$; $f_T$, unbound fraction in the cell; $f_u$, unbound fraction in plasma; I, inhibitor; $I_h$, concentration of inhibitor in the liver; $I_{in,max}$, maximum concentration of inhibitor in portal vein; $I_{in,max,u}$, maximum unbound concentration of inhibitor in the portal vein; $I_{in,u}$, unbound concentration of inhibitor in the portal vein; $I_{max}$, maximum concentration of inhibitor in the systemic blood; $I_{max,ss}$, steady–state maximum concentration of inhibitor; $I_{portal}$, concentration of inhibitor in portal vein; $I_{ss}$, steady–state total plasma concentration of inhibitor; $I_{sys}$, concentration of inhibitor in systemic blood; $I_u$, unbound concentration of the inhibitor; $k_a$, first order absorption rate constant; $k_{deg}$, degradation rate constant of the enzyme; $k_{el}$, elimination rate constant; $K_i$, inhibition constant; $K_{i,app}$, apparent inactivation constant; $k_{inact}$, maximum inactivation rate constant; $K_m$, Michaelis constant; $k_{obs}$, apparent inactivation rate constant; $K_p$, liver–to–blood concentration ratio; P, product; p–gp, p-glycoprotein; $P_{1,app}$, apparent influx clearance from the gut lumen into epithelial cells; $P_2$, efflux clearance from epithelial cells to the gut lumen; $P_3$, absorption clearance from the epithelial cells to the portal vein; PS, intrinsic clearance for membrane permeation; $PS_{active}$, membrane permeation clearance by active transport; $PS_{eff}$, intrinsic clearance for efflux; $PS_{inf}$, intrinsic clearance for influx; $PS_{passive}$, membrane permeation clearance by passive diffusion; $Q_a$, blood flow rate in the hepatic artery; $Q_h$, hepatic blood flow rate; $Q_{pv}$, blood flow rate in the portal vein; R, degree of inhibition; $R_c$, degree of increase in $C_{SS}$ and AUC; S, substrate; t′, time after oral administration; $t_{1/2}$, elimination half life; $t_{gi}$, small intestinal transit time; $T_{max}$, time to reach the maximum concentration; $V_{abs}$, absorption rate; $V_{av}$, average luminal volume; $V_d$, volume of distribution; $V_h$, volume of liver; $v_{in,max}$, maximum influx rate into the liver; $V_{max}$, maximum metabolic rate; $v_o$, initial uptake velocity obtained in the absence of ATP-depletors; $v_{passive}$, initial uptake velocity obtained in the presence of ATP-depletors; $V_{portal}$, volume of portal vein; $X_g$, change in gut extraction ratio; $X_h$, change in hepatic extraction ratio.

blood concentration caused by the redistribution of the drug into tissues, the unbound concentration is not affected. However, in the case of drugs with a small $V_d$, which depend on $f_u$ to a lesser extent, the total blood concentration is not affected so much by the change in $f_u$, but the unbound concentration is greatly altered.

Figure 1 shows the simulation of the effects of protein binding replacement on the blood concentration profile during a constant intravenous infusion, where the protein binding and the tissue distribution of the drug are assumed to reach equilibrium rapidly, i.e., the concentration changes rapidly in response to a change in $f_u$. In this simulation, changes in both CL and $V_d$ associated with the change in $f_u$ were considered. As just described above, the steady-state unbound concentration is altered with the change in $f_u$ only for a high clearance drug. It is also clear from figure 1 that, in the case of drugs with a small $V_d$, a transient increase in the unbound concentration is observed even for a low clearance drug, and caution for the possible occurrence of side effects is needed.

*B. Drug-drug interactions at the transport carrier*

Very few studies have focused on drug-drug interactions involving carrier-mediated transport across membranes, including the interactions involving renal secretion and reabsorption and those where p-glycoprotein (p-gp) plays a role (Tsuruo *et al.,* 1981; Slater *et al.,* 1986; Kusuhara *et al*., in press).

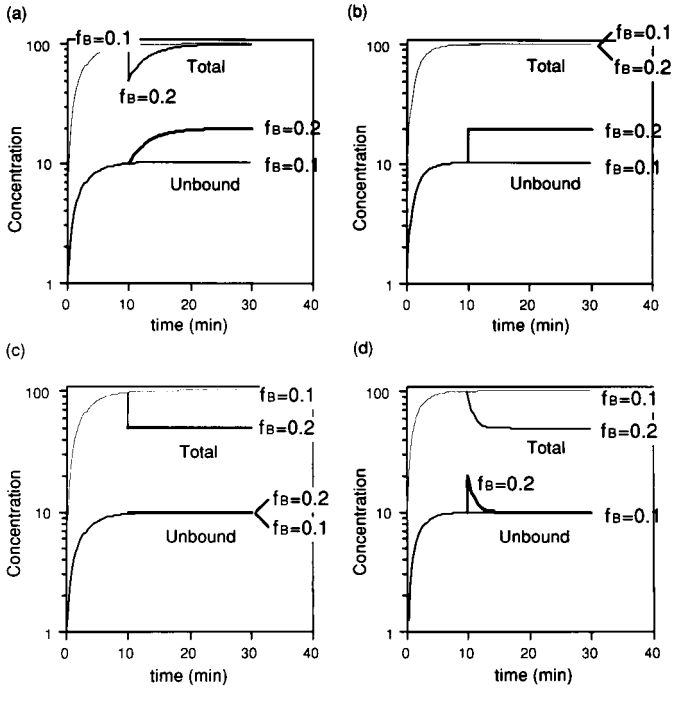


FIG. 1. Effects of protein binding replacement on the blood concentration profile during a constant intravenous infusion of (a) a high clearance drug with a high $V_d$, (b) a high clearance drug with a low $V_d$, (c) a low clearance drug with a high $V_d$, or (d) a low clearance drug with a low $V_d$. The protein binding and the tissue distribution of the drug are assumed to reach the equilibrium rapidly. An ideal situation is assumed where the concentration of the interacting drug (the displacer of the protein binding) immediately reaches a constant value at 10 min.

Along with metabolism, renal excretion is one of the most important processes affecting the total body clearance of a drug. Alterations in this process caused by drug-drug interactions should, therefore, be carefully considered. Secretion of drugs at the renal tubule is an active transport process, where organic anion transporters, organic cation transporters, and p-gp are known transport carriers (Hori *et al.,* 1982; Takano *et al.,* 1984; Tanigawara *et al.,* 1992). The renal clearance of a drug is reduced by inhibition of these transport processes. It is known that both organic anion transporters and organic cation transporters exist on both the basolateral membrane (BLM) and the brush border membrane (BBM) and that they are different from each other, whereas p-gp is only present on the BBM. The inhibitors of these transporters interact with other drugs; for example, inhibition of the renal excretion of penicillin and other related drugs by probenecid (Hunter, 1951), methotrexate excretion by nonsteroidal anti-inflammatory drugs (Statkevich *et al.,* 1993), and digoxin excretion by quinidine (Tanigawara *et al.,* 1992) all involve this kind of interaction.

Most studies of pharmacokinetic drug-drug interactions reported so far have been limited to the analysis of hepatic metabolism. However, the hepatic clearance of many drugs has been found to be determined mainly by hepatic uptake (Yamazaki *et al.,* 1995, 1996). The overall intrinsic clearance ($CL_{int,all}$) can be expressed using the intrinsic clearance for metabolism ($CL_{int}$) and that for membrane permeation (PS) as follows:

$$CL_{int,all} = PS_{inf} \cdot CL_{int}/(PS_{eff} + CL_{int}) \quad [1]$$

where $PS_{inf}$ is intrinsic clearance for influx, and $PS_{eff}$ is intrinsic clearance for efflux.

It is clear from equation (1) that $CL_{int,all}$ equals $CL_{int}$ in the case of drugs with large ($PS \gg CL_{int}$) and symmetrical ($PS_{inf} = PS_{eff}$) membrane permeability. Otherwise, hepatic clearance is affected by the membrane permeability of the drug. In such cases, it is important to evaluate drug-drug interactions involving not only metabolism but also membrane permeation. In our laboratory, several cases of drug-drug interactions were found in rats at the level of transporters involved in hepatobiliary transport as shown below. In the future, similar interactions at the transporter level possibly may be found in the clinical situation. The interactions found in rats include: inhibition of biliary excretion of glucuronides and sulfates of liquiritigenin, a flavonoid, by organic anions such as dibromosulfophthalein (DBSP) and glycyrrhizin, which has a glucuronide moiety (Shimamura *et al.,* 1994); inhibition of biliary excretion of glycyrrhizin by DBSP (Shimamura *et al.,* 1996); inhibition of biliary excretion of leukotriene $C_4$, which has a glutathione moiety, by DBSP (Sathirakul *et al.,* 1994);

and reduction of plasma clearance, based on hepatic uptake and biliary excretion, of octreotide, a small octapeptide, by DBSP and taurocholate (Yamada *et al.,* 1997). In vivo drug-drug interactions involving membrane transport remain to be predicted based on in vitro studies of the membrane permeability of drugs.

## III. Drug-Drug Interactions Involving Metabolism in the Liver

As a pharmacokinetic parameter directly related to the pharmacological and/or adverse effects of drugs, it is very important to predict the hepatic clearance. Because the use of animal scale-up is limited in the case of hepatic metabolic clearance due to large inherent interspecies differences, we have developed an alternative methodology to predict in vivo metabolic clearance in the liver; it is based on in vitro studies using mainly rat liver microsomes and isolated rat hepatocytes (Sugiyama and Ooie, 1993; Iwatsubo *et al.,* 1996). Recently, with the greater availability of human liver samples, the method of in vitro/in vivo scaling can now be applied to human studies. We have already demonstrated that the method can be applied to P450 metabolism in humans based on in vitro and in vivo data obtained from the literature (Iwatsubo *et al.,* 1997). However, the prediction of intrinsic clearance was not successful for some drugs, possibly because of the contribution of active transport into the liver and/or first-pass metabolism in the gut.

In order to prevent toxic drug-drug interactions, it is important to quantitatively predict pharmacokinetic changes caused by coadministration of drugs that are known to inhibit the hepatic metabolism of the drug under study (Sugiyama and Iwatsubo, 1996; Sugiyama *et al.,* 1996). In this review, we have focused on the drug-drug interactions via inhibitory mechanisms and have tried to predict in vivo interactions from in vitro data on drug metabolism obtained from the literature.

### *A. Examples of In Vivo Drug-Drug Interactions Involving P450 Metabolism*

Drug-drug interactions involving metabolism are one of the principal problems in clinical practice to evaluate the pharmacological and adverse effects of drugs. Parkinson (1996) summarized examples of substrates, inhibitors, and inducers of the major human liver microsomal P450 enzymes involved in drug metabolism. In the case of drugs that undergo metabolism by CYP3A4 and 2D6, particular attention should be paid to the interactions resulting in alterations in blood concentrations possibly accompanied by a change in its effects, because a number of drugs are metabolized by these enzymes (Bertz and Granneman, 1997). For example, blood concentrations of imipramine and desipramine, substrates for CYP2D6, are elevated several–fold by coadministration of fluoxetine, another substrate for CYP2D6 (Bergstrom *et al.,* 1992). Similarly, concentrations of terfenadine, which is metabolized by CYP3A4, are increased in patients taking erythromycin, which is also a substrate for CYP3A4 (Honig *et al.,* 1992). Quinidine is metabolized mainly by CYP3A4 but inhibits the metabolism of substrates for CYP2D6, such as sparteine, rather than those for CYP3A4 (Schellens *et al.,* 1991). Furthermore, in the case of drugs whose metabolism is mediated by multiple isozymes (e.g., diazepam), drug-drug interaction may be complicated because of possible dose-dependent changes in the contribution of each isozyme to the overall metabolism (Iwatsubo *et al.,* 1997).

### *B. Inhibition Mechanism of Drug Metabolism by P450*

Drug metabolism by P450 can be inhibited by any of the following three mechanisms.

The first is mutual competitive inhibition caused by coadministration of drugs metabolized by the same P450 isozyme, such as the above-mentioned (see Sec. A.) combinations of imipramine or desipramine and fluoxetine (CYP2D6). In this case, as reported for metoprolol and propafenone (CYP2D6) (Wagner *et al.,* 1987), blood concentrations of both drugs may be increased.

The second is the inactivation of P450 by the drug metabolite forming a complex with P450. This type of inhibition is designated as "mechanism-based inhibition" (Silverman, 1988). Inhibition by macrolide antibiotics, such as erythromycin, is a typical example of this type of interaction. As shown in figure 2, P450 demethylates and oxidizes the macrolide antibiotic into a nitrosoalkane that forms a stable, inactive complex with P450 (Periti *et al.,* 1992).

The third is inhibition by the binding of imidazole or a hydrazine group to the haem portion of P450. In the case of cimetidine, the nitrogen in the imidazole ring binds to the haem portion of P450 causing nonselective inhibition of many P450 isozymes (Somogyi and Muirhead, 1987).

### *C. Inhibition Patterns of Drug Metabolism*

The effects of inhibition of drug metabolism on in vivo pharmacokinetics are highly variable and depend on the properties of the drug, the route of administration, etc. (Rowland and Martin, 1973; Tucker, 1992). Except for

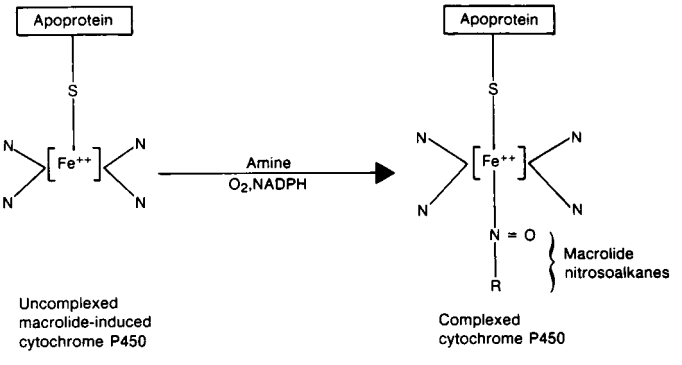


FIG. 2. Inhibition mechanism of P450 by macrolides (Periti *et al.,* 1992).

the case of mechanism-based inhibition, inhibition of drug metabolism can be classified into the following three categories, and the equations corresponding to each inhibition type have been derived (Todhunter, 1979).

*1. Competitive Inhibition.* Competitive inhibition is a pattern of the inhibition where the inhibitor competes with the drug for the same binding site within an enzyme protein:

$$E + S \rightleftarrows ES \rightarrow E + P$$

$K_m$ (Michaelis constant for S)

$$E + I \rightleftarrows EI$$

$K_i$ (Inhibition constant for I)

where E is the enzyme, S is the substrate, ES is the enzyme-substrate complex, P is the product, I is the inhibitor, and EI is the enzyme-inhibitor complex. In the case of competitive inhibition, the metabolic rate (v) can be expressed by the following equation (2):

$$v = \frac{V_{max} \cdot S}{K_m(1 + I/K_i) + S} \quad [2]$$

where $V_{max}$ is the maximum metabolic rate.

It is clear from equation (2) that the inhibition by a given concentration of I is marked when the substrate concentration is low and becomes less marked with an increase in the substrate concentration.

*2. Noncompetitive Inhibition.* Noncompetitive inhibition is a pattern of inhibition where the inhibitor binds to the same enzyme as the drug but the binding site is different, resulting in a conformation change, etc., of the protein:

$$\begin{aligned} E + S &\underset{K_m}{\rightleftarrows} ES \rightarrow E + P \\ E + I &\underset{K_i}{\rightleftarrows} EI \\ EI + S &\underset{K_m}{\rightleftarrows} EIS \\ ES + I &\underset{K_i}{\rightleftarrows} EIS \end{aligned}$$

where EIS is the enzyme-inhibitor-substrate complex. It is assumed that the inhibitor binds to the free enzyme and the ES complex with the same affinity. In the case of noncompetitive inhibition, the metabolic rate can be expressed by the following equation (3):

$$v = \frac{\{V_{max}/(1 + I/K_i)\} \cdot S}{K_m + S} \quad [3]$$

It is clear from equation (3) that the degree of inhibition does not depend on the substrate concentration.

*3. Uncompetitive Inhibition.* Uncompetitive inhibition is a pattern of inhibition where the inhibitor binds only to the enzyme forming a complex with the drug:

$$\begin{aligned} E + S &\underset{K_m}{\rightleftarrows} ES \rightarrow E + P \\ ES + I &\underset{K_i}{\rightleftarrows} EIS \end{aligned}$$

Unlike competitive and noncompetitive inhibition, the inhibitor cannot bind to the free enzyme. In the case of uncompetitive inhibition, the metabolic rate can be expressed by the following equation (4):

$$v = \frac{\{V_{max}/(1 + I/K_i)\} \cdot S}{K_m/(1 + I/K_i) + S} \quad [4]$$

It is clear from equation (4) that the inhibition becomes more marked with increasing substrate concentration.

The degree of inhibition depends on the inhibition pattern when the substrate concentration is high. However, when the substrate concentration is much lower than $K_m$ ($K_m \gg S$), the degree of inhibition (R) is expressed by the following equation (5), independent of the inhibition pattern, except in the case of the uncompetitive inhibition (Tucker, 1992):

$$R = \frac{v(+\text{inhibitor})}{v(-\text{inhibitor})} = \frac{1}{1 + I/K_i} \quad [5]$$

In clinical situations, the substrate concentration is usually much lower than $K_m$. In this review, we will discuss the most frequently observed case in which equation (5) can be applied.

### *D. Prediction of In Vivo Drug-Drug Interactions Based on In Vitro Data*

*1. General Equations.* The following factors determine the degree of change in $C_{ss}$ and AUC caused by the drug-drug interaction in vivo:

1) The route of administration (intravenous or oral, i.e., whether the drug first passes through the liver or not).
2) Fraction ($f_h$) of hepatic clearance ($CL_h$) in total clearance ($CL_{tot}$).
3) Fraction ($f_m$) of the metabolic process subject to inhibition in $CL_h$.
4) Unbound concentration of the inhibitor ($I_u$) around the enzyme.
5) Inhibition constant ($K_i$).
6) Plasma unbound concentration ($C_{u,ss}$) of the drug subject to inhibition.
7) Michaelis constant ($K_m$) for the drug subject to inhibition.

$f_h$ and $f_m$ are expressed as follows:

$$f_h = \frac{CL_h}{CL_h + CL_r} \quad [6]$$

$$f_m = \frac{CL_{int,1}}{CL_{int,1} + CL_{int,2}} \quad [7]$$

where $CL_h$ is hepatic clearance, $CL_r$ is renal clearance, and $CL_{int,1}$ and $CL_{int,2}$ represent the intrinsic clearance for the metabolic pathway inhibited and not inhibited by the inhibitor, respectively ($CL_{int} = CL_{int,1} + CL_{int,2}$). In equation (6), it is assumed that only the liver and kidney are the clearance organs. Equation (6) can be rearranged to give the following equation:

$$CL_r = CL_h(1/f_h - 1) \quad [8]$$

Equation (7) can be rearranged to give the following equation:

$$CL_{int,2} = CL_{int,1}(1/f_m - 1) \quad [9]$$

The fractional clearance for a particular metabolic pathway ($CL_{h,m}$) can be expressed as $f_h$ multiplied by $f_m$.

$R_c$, defined as the degree of increase in $C_{ss}$ and AUC caused by the drug-drug interaction in vivo, can be calculated as shown below, depending on the route of administration.

a. INTRAVENOUS ADMINISTRATION. The change in AUC after intravenous bolus administration ($AUC_{iv}$) and $C_{ss}$ during intravenous infusion can be expressed by the following equation, if the dose or infusion rate is constant:

$$\begin{aligned} R_c &= \frac{AUC_{iv}(+\text{inhibitor})}{AUC_{iv}(-\text{inhibitor})} = \frac{C_{ss}(+\text{inhibitor})}{C_{ss}(-\text{inhibitor})} \\ &= \frac{CL_{tot}}{CL_{tot}'} = \frac{CL_h + CL_r}{CL_h' + CL_r} = \frac{CL_h + CL_h(1/f_h - 1)}{CL_h' + CL_h(1/f_h - 1)} \\ &= \frac{CL_h/f_h}{CL_h' + CL_h/f_h - CL_h} = \frac{1}{f_h \cdot CL_h'/CL_h + 1 - f_h} \end{aligned} \quad [10]$$

where $'$ represents the value after alteration by the drug-drug interaction.

**i. High clearance drug.** Because $f_b \cdot CL_{int}$ is much larger than the hepatic blood flow rate ($Q_h$) ($Q_h \ll f_b \cdot CL_{int}$), $CL_h$ is rate-limited by the flow rate ($CL_h = Q_h$). When the altered $CL_h$ is still rate-limited by the flow rate ($CL_h' = Q_h$), i.e., $Q_h \ll f_b$. $CL_{int}'$, then $CL_h'$ equals $CL_h$. Thus, $R_c$ can be calculated to be unity by equation (10), indicating no change in $AUC_{iv}$ or $C_{ss}$. This is not the case when the inhibition is so extensive that $CL_h$ is not limited by the flow rate any more.

**ii. Low clearance drug.** In the case of a low clearance drug, $CL_h = f_b \cdot CL_{int}$ and $CL_h' = f_b$. $CL_{int}'$. If the protein binding is not altered by the inhibitor, the ratio (y) of $CL_h$ and $CL_h'$ can be calculated as follows:

$$\begin{aligned} y &= \frac{CL_h'}{CL_h} = \frac{f_b \cdot CL_{int}'}{f_b \cdot CL_{int}} = \frac{f_b \cdot (CL_{int}'_{,1} + CL_{int,2})}{f_b \cdot (CL_{int,1} + CL_{int,2})} \\ &= \frac{CL_{int}'_{,1} + CL_{int,1}(1/f_m - 1)}{CL_{int,1} + CL_{int,1}(1/f_m - 1)} \\ &= \frac{CL_{int}'_{,1} + CL_{int,1}/f_m - CL_{int,1}}{CL_{int,1}/f_m} \\ &= f_m \cdot CL_{int}'_{,1}/CL_{int,1} + 1 - f_m \end{aligned} \quad [11]$$

Combining equations (10) and (11) yields the following equation:

$$\begin{aligned} R_c &= \frac{1}{f_h(f_m \cdot CL_{int}'_{,1}/CL_{int,1} + 1 - f_m) + 1 - f_h} \\ &= \frac{1}{f_h \cdot f_m \cdot CL_{int}'_{,1}/CL_{int,1} + 1 - f_h \cdot f_m} \end{aligned} \quad [12]$$

Because $C_{u,ss}$ encountered clinically is usually much less than $K_m$, $CL_{int,1}$ and $CL_{int',1}$ can be expressed as follows:

$$CL_{int,1} = V_{max}/K_m \quad \text{and} \quad CL_{int}'_{,1} = V_{max}/K_m(1 + I_u/K_i)$$

where $I_u$ is the unbound concentration of the inhibitor. Therefore,

$$CL_{int}'_{,1}/CL_{int,1} = \frac{1}{1 + I_u/K_i} \quad [13]$$

can be derived. Combining equations (12) and (13) yields the following equation:

$$R_c = \frac{1}{f_h \cdot f_m \cdot \{1/(1 + I_u/K_i)\} + 1 - f_h \cdot f_m} \quad [14]$$

It is clear from equation (14) that, in the case of the intravenous administration of a low clearance drug, the degree of increase in $AUC_{iv}$ is determined not by $K_m$ or $C_{u,ss}$ but by $K_i$, $I_u$, $f_h$, and $f_m$, if $K_m \gg C_{u,ss}$.

b. ORAL ADMINISTRATION. The change in $AUC_{po}$ after a single oral administration and that in $C_{ss,av}$ after repeated oral administration can be expressed by the following equation (15), if the dose and administration interval is constant:

$$\begin{aligned} R_c &= \frac{AUC_{po}(+\text{inhibitor})}{AUC_{po}(-\text{inhibitor})} = \frac{C_{ss,av}(+\text{inhibitor})}{C_{ss,av}(-\text{inhibitor})} \\ &= \frac{CL_{oral}}{CL_{oral}'} = \frac{(CL_h + CL_r)/(F_h \cdot F_a)}{(CL_h' + CL_r)/(F_h' \cdot F_a)} \\ &= \frac{\{CL_h + CL_h(1/f_h - 1)\}/F_h}{\{CL_h' + CL_h(1/f_h - 1)\}/F_h'} \\ &= \frac{CL_h/f_h}{(CL_h' + CL_h/f_h - CL_h)} \cdot \frac{F_h'}{F_h} \\ &= \frac{1}{f_h \cdot CL_h'/CL_h + 1 - f_h} \cdot \frac{F_h'}{F_h} \end{aligned} \quad [15]$$

where $F_h$ is hepatic availability and $F_a$ is the fraction absorbed from the gastrointestinal tract into the portal vein.

Some kind of mathematical model has to be introduced for the calculation of the hepatic intrinsic clearance ($CL_{int}$) in vivo. In order to avoid a false negative prediction of drug-drug interactions, we tried to evaluate the maximum inhibitory effect expected. The well-stirred model was selected as one which can detect the maximum effect of the inhibitor. In the case of oral

administration where D is dose, $D/AUC_{po} = D/\tau/C_{ss,av} = CL_h/F_h = f_b \cdot CL_{int}$ can be derived based on the well-stirred model, irrespective of the value of $CL_h$ relative to $Q_h$, where D is dose. In this model, therefore, either $AUC_{po}$ or $C_{ss,av}$ is affected directly by the reduction in $CL_{int}$ without a contribution from the hepatic blood flow rate. For this reason, the well-stirred model can detect the maximum effect of an inhibitor. Thus, the well-stirred model was used in the following discussion of the prediction of drug-drug interactions after oral administration.

**i. High clearance drug.** Because $f_b \cdot CL_{int}$ is much larger than the hepatic blood flow rate ($Q_h \ll f_b \cdot CL_{int}$), $CL_h$ is rate-limited by the flow rate ($CL_h = Q_h$). When the altered $CL_h$ is still rate-limited by the flow rate ($CL_h' = Q_h$), i.e., $Q_h \ll f_b \cdot CL_{int}'$, then $CL_h'$ equals $CL_h$. On the other hand, $F_h = Q_h/(f_b \cdot CL_{int})$ and $F_h' = Q_h/(f_b \cdot CL_{int}')$. Therefore, the following equation (16) can be derived from equation (15):

$$R_c = \frac{F_h'}{F_h} = \frac{CL_{int}}{CL_{int}'} = \frac{CL_{int,1} + CL_{int,2}}{CL_{int}'_{,1} + CL_{int,2}}$$

$$= \frac{CL_{int,1} + CL_{int,1}(1/f_m - 1)}{CL_{int}'_{,1} + CL_{int,1}(1/f_m - 1)} \qquad [16]$$

$$= \frac{CL_{int,1}/f_m}{CL_{int}'_{,1} + CL_{int,1}/f_m - CL_{int,1}}$$

$$= \frac{1}{f_m \cdot CL_{int}'_{,1}/CL_{int,1} + 1 - f_m}$$

Furthermore, as $C_{u,ss}$ encountered clinically is usually much less than $K_m$, $CL_{int,1}$ and $CL_{int}'_{,1}$ can be expressed as follows:

$$CL_{int,1} = V_{max}/K_m \quad \text{and} \quad CL_{int}'_{,1} = V_{max}/K_m(1 + I_u/K_i)$$

Therefore,

$$CL_{int}'_{,1}/CL_{int,1} = \frac{1}{1 + I_u/K_i} \qquad [17]$$

can be derived. Combining equations (16) and (17) yields the following equation:

$$R_c = \frac{1}{f_m \cdot \{1/(1 + I_u/K_i)\} + 1 - f_m} \qquad [18]$$

**ii. Low clearance drug.** Since the first-pass hepatic availability is close to unity for low clearance drugs, the final equation (14) should be the same for intravenous and oral administration.

The effect of the inhibitor on the $C_{max}$ after oral administration also depends on the clearance of the drug. Assuming that the drug absorption from the gastrointestinal tract is sufficiently rapid, $C_{max}$ is proportional to $F_h$. Based on the well–stirred model, $F_h$ can be expressed as follows:

$$F_h = Q_h/(Q_h + f_b \cdot CL_{int}) \qquad [19]$$

It is clear from equation (19) that $F_h$ is minimally affected by the change in $CL_{int}$ in the case of a low clearance drug ($Q_h \gg f_b \cdot CL_{int}$: $F_h = 1$), but is inversely proportional to $CL_{int}$ in the case of a high clearance drug ($Q_h \ll f_b \cdot CL_{int}$: $F_h = Q_h/f_b \cdot CL_{int}$), in which case $C_{max}$ also changes in inverse proportion to $CL_{int}$.

In summary, it is important to know the values of $K_i$, $I_u$, $f_h$, and $f_m$ in order to predict in vivo drug-drug interactions. Approximated $f_h$ and $f_m$ values can be estimated from the urinary recovery of the parent compound and each metabolite. $K_i$ values can be evaluated by kinetic analysis of in vitro data using human liver microsomes and recombinant systems and this has already been done for many compounds. The key, therefore, is the evaluation of $I_u$.

*2. The evaluation of the unbound concentration of the inhibitor in vivo.* Although $I_u$ is the unbound concentration of the inhibitor around the metabolic enzyme in the liver, it is impossible to directly measure this in vivo. However, many drugs are transported into the liver by passive diffusion, allowing for the assumption that the unbound concentration in the liver equals that in the liver capillary at steady-state. This means that estimating the unbound concentration of the inhibitor in the liver capillary may be enough for some drugs. This assumption is not valid, however, in the case of drugs which are actively transported into or out of the liver; the unbound concentration in the liver may be higher in the former case or lower in the latter than in the liver capillary (fig. 3). In these cases, another experiment using human hepatocytes, human liver slices, etc., is required to estimate the kinetic parameters for the active transport. Furthermore, the unbound concentration in the liver capillary is always changing and a concentration gradient is formed from the entrance (portal vein) to the exit (hepatic vein). Which of these concentrations should be considered as $I_u$? An underestimation of $I_u$ may lead to a "false negative" prediction of actually

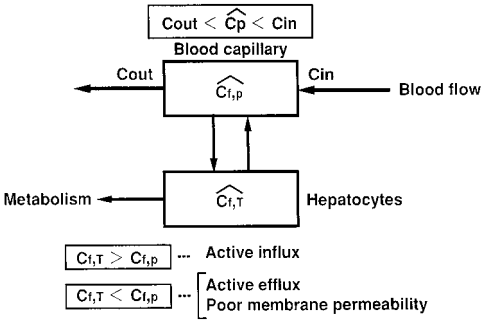


FIG. 3. Relationship between unbound drug concentration in the liver capillary ($C_{f,p}$) and that in the liver ($C_{f,T}$). $C_{in}$ and $C_{out}$ represent the drug concentration at the entrance (portal vein side) and the exit (hepatic vein side) of the liver, respectively.

occurring in vivo drug interaction from in vitro data. In order to avoid a false negative prediction caused by underestimation of $I_u$, the plasma unbound concentration at the entrance to the liver, where the blood flow from the hepatic artery and portal vein meet, was considered the maximum value of $I_u$ and was used in the prediction ($I_{in,u}$; fig. 4).

Practically, the maximum plasma concentration in the circulation ($I_{max}$) has been estimated for many inhibitors. When the value of $I_{max}$ is not reported, it can be predicted from both the plasma concentration at a single time point after administration and the pharmacokinetic parameters such as the elimination half life ($t_{1/2,\beta}$).

According to the model in figure 4, influx into the liver consists of contributions from the hepatic artery and portal vein (after gastrointestinal absorption). When the drug is absorbed from the gastrointestinal tract with a first-order rate constant ($k_a$), the maximum influx rate into the liver ($v_{in,max}$) can be expressed as follows:

$$v_{in,max} \leqq Q_a I_{max} + Q_{pv} I_{max} + k_a \cdot D \cdot F_a \cdot e^{-kat'} \quad [20]$$

where $Q_a$ and $Q_{pv}$ represent the blood flow rate in the hepatic artery and the portal vein, respectively, $F_a$ is the fraction absorbed from the gastrointestinal tract into the portal vein, and $t'$ is the time after oral administration (after subtraction of the lag-time).

When the absorption rate is maximum (i.e., $t' = 0$), the final term in equation (20) can be expressed as $k_a \cdot D \cdot F_a$ and thus:

$$v_{in,max} \leqq (Q_a + Q_{pv}) I_{max} + k_a \cdot D \cdot F_a \quad [21]$$

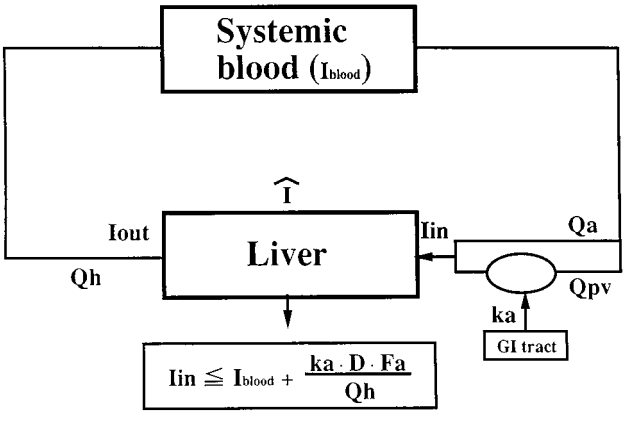


FIG. 4. Model for estimating inflow concentration of the inhibitor into the liver after oral administration ($I_{in}$). $I_{out}$, I, and $I_{blood}$ represent the inhibitor concentration at the exit of liver (hepatic vein side), the inhibitor concentration at the liver capillary, and inhibitor concentration in the systemic circulation, respectively. $Q_a$, $Q_{pv}$ and $Q_h$ ($=Q_a + Q_{pv}$) represent blood flow at hepatic artery, portal vein, and hepatic vein, respectively. $k_a$, D, and $F_a$ represent the absorption rate constant, dose, and the fraction absorbed from the gastrointestinal tract into the portal vein, respectively, of the inhibitor.

As $Q_h = Q_a + Q_{pv}$, the following equation can be derived:

$$I_{in,max} = v_{in,max}/Q_h = \underbrace{I_{max}}_{\text{Contribution from the systemic circulation}} + \underbrace{(k_a \cdot D/Q_h) \cdot F_a}_{\text{Contribution from the absorption}} \quad [22]$$

Therefore, $I_{in,max}$ can be predicted if the parameters such as $k_a$ and $F_a$ are available for the inhibitor. Taking the plasma protein binding into consideration, the unbound $I_{in,max}$ ($I_{in,max,u}$) can be calculated as $I_{in,max} \cdot f_u$. Finally, comparing the value of $I_{in,max,u}$ as $I_{in,u}$ and that of $K_i$ obtained in vitro allows the prediction of the maximum degree of in vivo drug-drug interaction caused by metabolic inhibition.

In general, the apparent absorption rate of the orally administered drug is maximum when the gastrointestinal absorption of the drug is so rapid that the rate-limiting step is the gastric emptying rate. A first order rate constant ($k_a$) of about 0.1 $min^{-1}$ is reported for gastric emptying in rats and humans (Oberle *et al.,* 1990). On the other hand, the absorption rate constant in humans can be calculated from the time to reach the maximum concentration ($T_{max}$) and the elimination constant ($k_{el}$) as follows:

$$T_{max} = ln(k_a/k_{el})/(k_a - k_{el}) \quad [23]$$

In practice, however, because of the possible estimation error of $T_{max}$ caused by interindividual differences etc., the calculated value of $k_a$ sometimes exceeds 0.1 $min^{-1}$, though it should never exceed that, theoretically, for gastric emptying. Therefore, the theoretically maximum value of 0.1 $min^{-1}$ was used for $k_a$ when it was calculated to be larger than 0.1 $min^{-1}$. Moreover, in order to avoid a false negative prediction, the maximum $k_a$ of 0.1 $min^{-1}$ was used to obtain the largest inhibitor concentration if $k_a$ was unknown.

### *E. Examples of the Prediction of Drug-Drug Interactions Based on Literature Data*

The methodology described above (see Section III.D.) has been applied to the prediction of in vivo drug-drug interactions from in vitro data gathered from the literature.

*1. Successful Cases of In Vitro/In Vivo Prediction.* a. TOLBUTAMIDE-SULFAPHENAZOLE. Interactions between tolbutamide and sulfa-agents cause serious side effects such as hypoglycemic shock in patients (Christensen *et al.,* 1963) and exhibit the marked interspecies differences in animals. Veronese *et al.* (1990) reported about a five-fold increase in both $AUC_{po}$ and $t_{1/2}$ of tolbutamide in humans following coadministration of 500 mg sulfaphenazole (table 2, fig. 5).

The $t_{1/2}$ of intravenous tolbutamide is prolonged and the $CL_{tot}$ is reduced markedly in rats, too, by sulfa-

TABLE 2
*Inhibition of tolbutamide metabolism (CYP2C9) by coadministration of sulfaphenazole*

| | Dose (mg) | Route | AUC (ng · hr/ml) | $CL_{tot}$ (ml/min) | |
|---|---|---|---|---|---|
| control | 500 | p.o. | 587 | 27.5 | |
| + sulfaphenazole | | | 3100 | | |
| | $CL_r$ (ml/min) | $CL_h$ (ml/min) | $CL_{h,m}$[a] (ml/min) | $CL_{h,m}/CL_{tot}$ | $I_{in,u}/K_i$ |
| | 0.42 | 27.1 | 21.7 | 0.8 | 125–250 |

[a] methyl hydroxylation (2C9)+carboxylation (sequential).

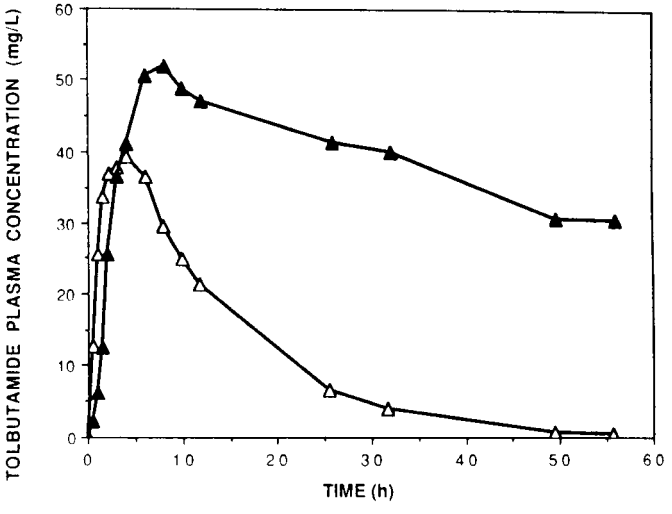


FIG. 5. Effect of sulfaphenazole coadministration on plasma concentration of tolbutamide (Veronese *et al.,* 1990). △: Tolbutamide (500 mg p.o.) alone; ▲: Tolbutamide (500 mg p.o.)+Sulfaphenazole (500 mg p.o., q12h).

phenazole (Sugita *et al.,* 1981). On the contrary, the $CL_{tot}$ of tolbutamide is increased 15 to 30% in rabbits with little change in the $t_{1/2}$ (fig. 6) (Sugita *et al.,* 1984). Because tolbutamide is a low clearance drug with a small urinary excretion, the $CL_{tot}$ after intravenous administration is expressed by the following equation (24):

$$CL_{tot} = D/AUC = f_b \cdot CL_{int} \quad [24]$$

Sugita *et al.* (1984) tried to reconstruct the $CL_{tot}$ in vivo based on the values of unbound fraction in blood ($f_b$) and $CL_{int}$ estimated separately by in vitro binding and metabolic studies. Sulfaphenazole inhibits both plasma protein binding and hepatic metabolism of tolbutamide, causing the increase in $f_b$ and the reduction in $CL_{int}$, in both species. Although the $CL_{int}$ falls to about one-fourth and the $f_b$ increases about two-fold in rats, resulting in about a half-fold reduction in the $CL_{tot}$, the $CL_{int}$ falls to about one-half and the $f_b$ increases about two-fold in rabbits resulting in little change in the $CL_{tot}$ (fig. 7). The effects on the $CL_{int}$ and $f_b$ of tolbutamide are not constant among sulfa-agents; sulfadimethoxine also reduces the $CL_{int}$ by about one-half in rabbits but increases the $f_b$ more than two-fold, resulting in an increase in the $CL_{tot}$ and a reduction in the AUC (Sugita *et al.,* 1984).

The interaction between tolbutamide and sulfaphenazole involves both plasma protein binding and hepatic metabolism in humans, too. The main metabolic pathway of tolbutamide in vitro is CYP2C9-mediated hydroxylation, and the metabolite undergoes sequential metabolism forming a carboxylate in vivo (Thomas and Ikeda, 1966; Nelson and O'Reilly, 1961). The $K_i$ of sulfaphenazole, a specific inhibitor of CYP2C9, for tolbutamide methyl hydroxylation in human liver microsomes in vitro is 0.1–0.2 $\mu$M (Miners *et al.,* 1988; Back *et al.,* 1988). The $I_{max}$ of sulfaphenazole after a 500 mg dose was 70 $\mu$M in humans, and the absorption term [the second term in equation (22)] was calculated to be 8.0 $\mu$M using $k_a = 0.0095\ min^{-1}$, D = 500 mg, $Q_h$ = 1610 ml/min, and $F_a = 0.85$. $I_{in,max}$ was, therefore, calculated to be 78 $\mu$M, indicating that the contribution of systemic circulation is greater than that of absorption. Taking the $f_u$ value (0.32) of sulfaphenazole into consideration, $I_{in,u}/K_i$ was calculated to be 125–250 (table 2). The plasma protein binding of tolbutamide is also inhibited by sulfaphenazole in humans, resulting in about a three-fold increase in $f_b$ (Christensen *et al.,* 1963). However, the inhibition is considered almost complete in terms of the product of $f_b$ and $CL_{int}$ because the extent of inhibition of metabolism is much greater than that of its plasma protein binding. The contribution of the CYP2C9-related metabolic pathway of tolbutamide is about 80% of the total ($f_h \cdot f_m = CL_{h,m}/CL_{tot} = 0.8$) (table 2). Therefore, complete inhibition of this metabolic pathway leads to an 80% reduction in $CL_{int}$, and the $AUC_{po}$ is predicted to be five times larger than the control value, which is consistent with the observed increase (table 2).

b. TRIAZOLAM-KETOCONAZOLE. Von Moltke *et al.* (1996) reported that plasma triazolam concentration after oral administration of 0.125 mg was greatly elevated by oral ketoconazole (200 mg), producing a nearly nine-fold reduction in the apparent oral clearance. They predicted this interaction based on in vitro studies using human liver microsomes (table 3). Triazolam is eliminated in humans mainly by CYP3A-mediated metabolism to $\alpha$-hydroxy (OH)- and 4-OH-triazolam. Ketoconazole is a powerful inhibitor of both these metabolic pathways, with a mean $K_i$ value of 0.006 and 0.023 $\mu$M, respectively (Von Moltke *et al.,* 1996). In order to estimate ketoconazole concentrations in the liver, they conducted an in vitro study using mouse liver homogenates in human plasma spiked with ketoconazole; a liver/plasma partition ratio of 1.12 was obtained. On the other hand,

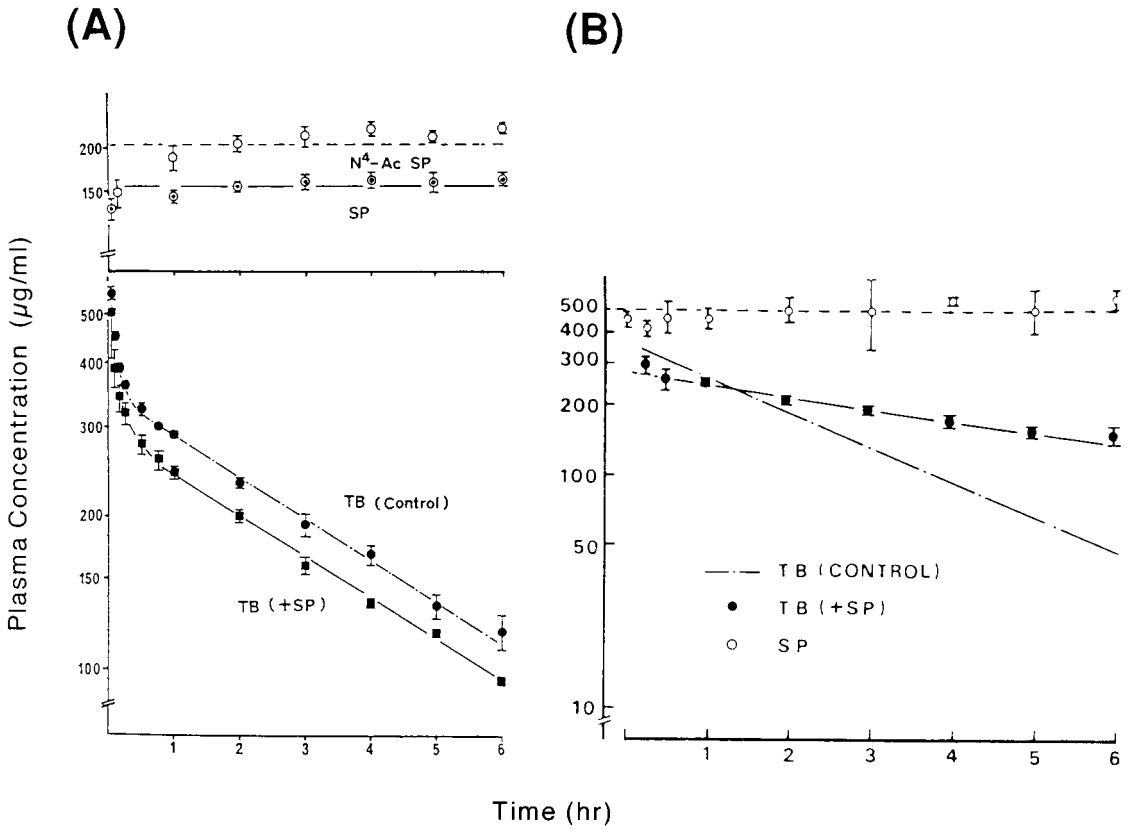


FIG. 6. Effect of sulfaphenazole (SP) coadministration on plasma concentration of tolbutamide (TB) in rabbits (A) and rats (B) (Sugita *et al.,* 1981, 1984). Open and closed symbols represent plasma concentrations of sulfaphenazole (or its metabolite, N4-Ac SP) and tolbutamide, respectively.

the partition ratio was calculated to be 2.03 in the in vivo mouse study where the ketoconazole concentrations in plasma and liver were measured. The concentration of ketoconazole in the liver was estimated by multiplying this partition ratio by the total ketoconazole concentration in plasma in the clinical study (0.04–9.32 $\mu$M). Using the in vitro $K_i$ values, ketoconazole concentration in the liver, and the contribution of both metabolic pathways (52.5% and 47.5% for $\alpha$- and 4-OH-pathway, respectively), the predicted degree of reduction (>95%) in triazolam clearance in vivo was consistent with the 88% reduction actually observed in vivo (table 3). However, it should be noted that in this report, the total concentration of the inhibitor was used instead of unbound concentration in the liver. The unbound concentration needs to be estimated because the $K_i$ values obtained in the in vitro studies are based on the concentration in the medium.

Using our method proposed above (see Section III.D.), the ketoconazole-triazolam interaction would be predicted as follows: The $I_{max,ss}$ of ketoconazole during administration of 200 mg×2/day was 6.6 $\mu$M (Daneshmend *et al.,* 1981), and the absorption term [the second term in equation (22)] was calculated to be 1.4–2.5 $\mu$M using $k_a$ = 0.0099–0.018 $min^{-1}$, D = 200 mg, $Q_h$=1610 ml/min, and $F_a$ = 0.59. The $k_a$ was calculated from equation (23) using the values of $T_{max}$ and $t_{1/2}$ (=0.693/$k_{el}$) (Daneshmend *et al.,* 1984). The $I_{in,max}$ is, therefore, calculated to be 8.0–9.1 $\mu$M. Since the $f_u$ of ketoconazole is 0.01, the $I_{in,max,u}$ is calculated to be 0.080–0.091 $\mu$M and the obtained $I_{in,max,u}/K_i$ value is 13–15 and 3.5–4.0 for the $\alpha$-OH and 4-OH pathways, respectively, using a $K_i$ value of 0.006 and 0.023 $\mu$M, respectively. Therefore, the reduction in the clearance can be estimated as follows, considering the contribution of each pathway to the total metabolism:

$$R = \frac{1}{1 + (13\text{–}15)} \times 0.525 + \frac{1}{1 + (3.5\text{–}4.0)} \times 0.475$$

$$= 0.128\text{–}0.143$$

Thus, an 85.7–87.2% reduction is predicted by this method, which is very close to the observed reduction (88%) (table 3). The degree of the inhibition should be larger if ketoconazole is actively transported into the liver.

Two cases have been shown here in which the interaction that had actually occurred in vivo was successfully predicted based on in vitro metabolism data. On the other hand, we believe that the ability to predict by the above-mentioned methods based on in vitro data should be very high in the case of drug combinations that do not interact with each other in vivo. In other words, the absence of in vivo drug-drug interactions should be successfully predicted, which has been partly

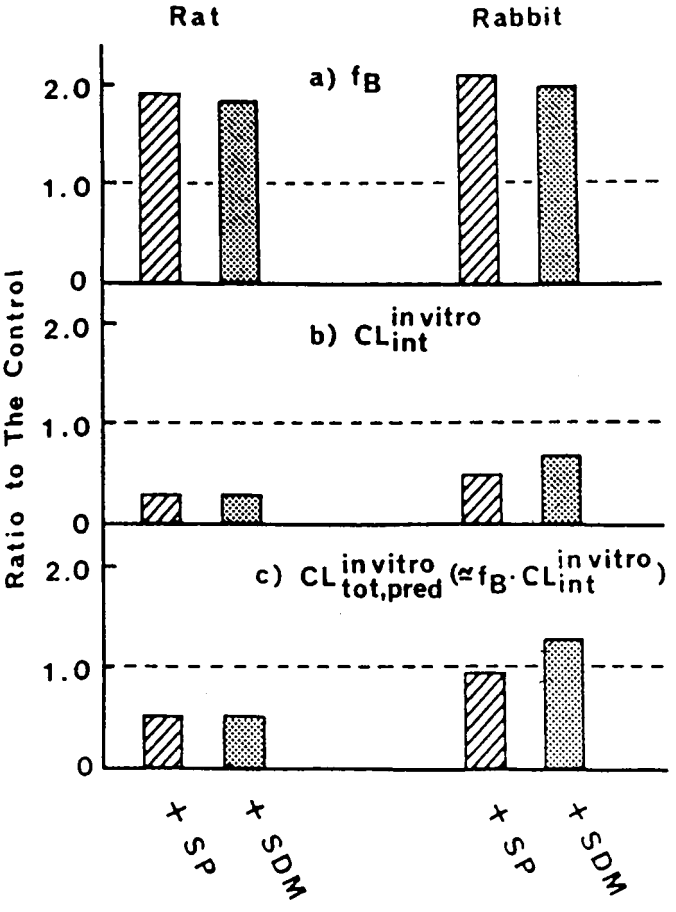


FIG. 7. Prediction of interspecies difference in the interaction of tolbutamide and sulfaphenazole (SP) or sulfadimethoxine (SDM) from in vitro data (Sugita *et al.,* 1984).

confirmed in our study, though the data are not shown here.

*2. Interactions Predictable for the Objective Metabolic Pathway but not Predictable for the Overall Data.* a. SPARTEINE-QUINIDINE. Schellens *et al.* (1991) reported that the $CL_{oral}$ of sparteine (dose: 50 mg) fell from 979 to 341 ml/min (35% of the control value) after coadministration of 200 mg quinidine (table 4). The main metabolic pathway of sparteine is CYP2D6-mediated dehydration. Because quinidine is a specific inhibitor of CYP2D6, it is reasonable that metabolic inhibition is involved in this quinidine-induced reduction in the $CL_{oral}$ of sparteine. The $K_i$ of quinidine for the CYP2D6-mediated metabolism in human liver microsomes in vitro is reported to be 0.06 $\mu$M. The $I_{max}$ of quinidine after a dose of 200 mg was 4.1 $\mu$M, and the absorption term [the second term in equation (22)] was calculated to be 0.86–22 $\mu$M using $k_a = 0.0027–0.069\ min^{-1}$, D = 200 mg, $Q_h$ = 1610 ml/min, and $F_a$ = 0.83. $I_{in,max}$ is, therefore, calculated to be 5–26 $\mu$M. Because the $f_u$ of quinidine is 0.15, the $I_{in,u}$ and $I_{in,u}/K_i$ are calculated to be 0.75–3.9 $\mu$M and 13–65, respectively (table 4). Thus, it was predicted that the dehydration pathway of sparteine would be almost completely inhibited by quinidine. The contribution of the dehydration pathway of sparteine to the total elimination is about 25% ($f_h \cdot f_m = CL_{h,m}/CL_{tot} = 0.25$) (table 4). Therefore, the complete inhibition of this dehydration pathway will reduce the $CL_{oral}$ to 75% of the control value, which is about two-fold larger than the observed reduction to 35%. The reasons for this discrepancy may include the possibility that metabolic pathways other than dehydration may also be inhibited by quinidine.

TABLE 3
*Comparison of the prediction of triazolam-ketoconazole interaction by von Moltke's and our method*

| | | Our method | von Moltke's method |
|---|---|---|---|
| $K_i$ ($\mu$M) | $\alpha$-OH | 0.006 | 0.006 |
| | 4-OH | 0.023 | 0.023 |
| $I_{plasma}$ ($\mu$M) | | 8.0–9.1 | 9.32 |
| $I_{liver}$ ($\mu$M) | | — | 10.4–18.9 ($K_p$ = 1.12–2.03) |
| $Iu_{liver}$ (=$Iu_{plasma}$) ($\mu$M) | | 0.080–0.091 | — |
| $I_{liver}/K_i$ | $\alpha$-OH | — | 1730–3150 |
| | 4-OH | — | 452–822 |
| $Iu_{liver}/K_i$ | $\alpha$-OH | 13–15 | — |
| | 4-OH | 3.5–4.0 | — |
| Predicted degree of inhibition | | 86–87% | >95% |

b. TERFENADINE-KETOCONAZOLE. Honig *et al.* (1993) reported that blood concentrations of terfenadine (dose: 60 mg), detectable only in one of six subjects when administered alone ($I_{max}$ = 7 ng/ml), became detectable in all subjects following coadministration of 200 mg ketoconazole, with the highest $I_{max}$ in the same subject elevated to 81 ng/ml (table 5). The main elimination pathway of terfenadine is CYP3A4-mediated N-dealkylation and hydroxylation yielding a carboxylate, which may undergo sequential N-dealkylation (Garteiz *et al.,* 1982). $K_i$ values of ketoconazole for terfenadine metabolism in vitro have been reported by two groups. Jurima-Romet *et al.* (1994) reported the $K_i$ values of 3 and 10 $\mu$M in human liver microsomes and <1 and 3 $\mu$M in human hepatocytes (Jurima-Romet *et al.,* 1996; Li *et al.,* 1997) for the N-dealkylation and hydroxylation pathways, respectively. Based on the $K_i$ values in human liver microsomes reported by Von Moltke *et al.* (1994), $I_{in,u}/K_i$ value was calculated to be 3.3–3.8 and 0.33–0.38 for the N-dealkylation and hydroxylation pathways, respectively (table 5) [see our previous review (Ito *et al.,* 1998) for the details]. As the estimated contribution ($f_h \cdot f_m = CL_{h,m}/CL_{tot}$) of these two pathways to the total metabolism was about 0.13 and 0.45, respectively, the increase in the availability and $C_{max}$ caused by the metabolic inhibition was predicted to be about 1.3-fold according to equation (14). However, the $C_{max}$ was actually increased more than 10-fold. The possible reasons to explain this great discrepancy include: inaccurate measurements of clinical concentrations of terfenadine being around the detection limit of the assay, and the contribution of the other 50% of the metabolism of terfenadine neglected in the analysis. As shown later (see Section III.H.2.), interactions involving metabolism and/or efflux process in the gut may have some con-

TABLE 4
*Inhibition of sparteine metabolism (CYP2D6) by coadministration of quinidine*

| | Dose (mg) | Route | AUC (ng · hr/ml) | $CL_{tot}$ (ml/min) | |
|---|---|---|---|---|---|
| control | 50 | p.o. | 851 | 514 | |
| + quinidine | | | | 2440 | |
| | $CL_r$ (ml/min) | $CL_h$ (ml/min) | $CL_{h,m}$[a] (ml/min) | $CL_{h,m}/CL_{tot}$ | $I_{in,u}/K_i$ |
| | 154 | 360 | 126 | 0.25 | 13–65 |

[a] dehydration.

TABLE 5
*Inhibition of terfenadine metabolism (CYP3A4) by coadministration of ketoconazole*

| | Dose (mg) | Route | $C_{max}$ (ng/ml) | $CL_{tot}$ (ml/min) | |
|---|---|---|---|---|---|
| control | 60 | p.o. | <7 | 84300 | |
| + ketoconazole | | | | 81 | |
| | $CL_r$ (ml/min) | $CL_h$ (ml/min) | $CL_{h,m}$ (ml/min) | $CL_{h,m}/CL_{tot}$ | $I_{in,u}/K_i$ |
| | negligible | 84300 | 11000[a], 37900[b] | 0.13[a], 0.45[b] | 3.3–3.8[a]<br>0.33–0.38[b] |

[a] the values for N-dealkylation.
[b] the values for hydroxylation.

TABLE 6
*Inhibition of imipramine metabolism (CYP2D6) by coadministration of fluoxetine*

| | Dose (mg) | Route | AUC (ng · hr/ml) | $CL_{tot}$ (ml/min) | |
|---|---|---|---|---|---|
| control | 50 | p.o. | 372 | 537 | |
| + fluoxetine | | | | 703 | |
| | $CL_r$ (ml/min) | $CL_h$ (ml/min) | $CL_{h,m}$[a] (ml/min) | $CL_{h,m}/CL_{tot}$ | $I_{in,u}/K_i$ |
| | negligible | 537 | 96.7 | 0.18 | 0.066 |

[a] 2-hydroxylation.

tributions in the in vitro/in vivo discrepancy. If the value of $I_{in,u}/K_i$ comparable to that for N-dealkylation (3.8) can be applied to other metabolic pathways, the AUC is predicted to increase more than five-fold, which is close to the results in vivo.

*3. Interactions Not Predictable by In Vitro/In Vivo Scaling.* a. IMIPRAMINE-FLUOXETINE. Coadministration of tricyclic antidepressants such as imipramine and desipramine with fluoxetine may induce severe side effects including delirium and grand mal seizure (Preskorn *et al.,* 1990). The $AUC_{po}$ of imipramine (dose: 50 mg) is reported to increase about 1.9-fold after coadministration of 60 mg fluoxetine (table 6) (Bergstrom *et al.,* 1992). The main elimination pathways of imipramine are 2-hydroxylation and N-demethylation yielding desipramine, which undergoes further 2-hydroxylation. The 2-hydroxylation pathway is mainly catalyzed by CYP2D6. On the other hand, fluoxetine is a specific inhibitor of CYP2D6 with a $K_i$ of 0.92 $\mu$M for the 2-hydroxylation of imipramine in human liver microsomes (Skjelbo and Brosen, 1992). The $I_{max}$ of fluoxetine after administration of 60 mg is 0.2 $\mu$M (Aronoff *et al.,* 1984), and the absorption term [the second term in equation (22)] was calculated to be 0.83 $\mu$M using $k_a = 0.012\ min^{-1}$, D = 60 mg, $Q_h$ = 1610 ml/min, and $F_a$ = 0.80. The $k_a$ was calculated from equation (23) using the values of $T_{max}$ and $t_{1/2}$(=0.693/kel). Therefore, the $I_{in,max}$ is 1.02 $\mu$M, indicating that absorption makes a major contribution. Because the $f_u$ of fluoxetine is 0.06, the $I_{in,u}$ and $I_{in,u}/K_i$ are calculated to be 0.061 $\mu$M and 0.066, respectively (table 6). Furthermore, the contribution ($f_h \cdot f_m = CL_{h,m}/CL_{tot}$) of this metabolic pathway (2-hydroxylation) is about 18% of the total. According to equation (14), therefore, the metabolic inhibition in vivo was not predicted to have a significant effect on the AUC in spite of the approximately 2-fold increase actually observed (table 6). Possible reasons for this discrepancy include the estimation error of $K_i$ and the possibility that other metabolic pathways and pharmacokinetic processes also may be altered by fluoxetine.

b. CAFFEINE-CIPROFLOXACIN. Stille *et al.* (1987) reported that the $AUC_{po}$ of caffeine (dose: 220 to 230 mg) increased about 1.6-fold after coadministration of 250 mg ciprofloxacin (table 7). The main metabolic pathways of caffeine are 1-demethylation, 3-demethylation, 7-demethylation, and 8-hydroxylation, mediated by CYP1A2. Because antimicrobial agents such as ciprofloxacin are specific inhibitors of CYP1A2, metabolic inhibition should be involved in the ciprofloxacin-induced increase in the $AUC_{po}$ of caffeine. The $K_i$ of ciprofloxacin for caffeine 3-demethylation in human liver microsomes in vitro is around 150 $\mu$M (Kalow and Tang, 1991). The $I_{max}$ of ciprofloxacin after administration of 250 mg is 4.3–6.0 $\mu$M (Guay *et al.,* 1987), and the absorption term [the second term in equation (22)] was

TABLE 7
*Inhibition of caffeine metabolism (CYP1A2) by coadministration of ciprofloxacin*

| | Dose (mg) | Route | AUC (ng · hr/ml) | $CL_{tot}$ (ml/min) | |
|---|---|---|---|---|---|
| control | 220–230 | p.o. | 22.4 | 84.0 | |
| + ciprofloxacin | | | 35.2 | | |
| | $CL_r$ (ml/min) | $CL_h$ (ml/min) | $CL_{h,m}$ [a] (ml/min) | $CL_{h,m}/CL_{tot}$ | $I_{in,u}/K_i$ |
| | negligible | 84.0 | 66.4 | 0.79 | 0.07–0.15 |

[a] 1-demethylation+3-demethylation+7-demethylation+8-hydroxylation.

calculated to be 9.3–22 $\mu$M using $k_a = 0.02–0.04\ min^{-1}$, D = 250 mg, $Q_h$ = 1610 ml/min, and $F_a$ = 0.92. Therefore, the $I_{in,max}$ was calculated to be 14–28 $\mu$M, indicating that the contribution of absorption is greater than that of the systemic circulation. Because the $f_u$ of ciprofloxacin is 0.8, the $I_{in,u}$ and $I_{in,u}/K_i$ are calculated to be 11–22 $\mu$M and 0.07–0.15, respectively (table 7). The contribution ($f_h \cdot f_m = CL_{h,m}/CL_{tot}$) of this pathway to the total elimination is about 79% (table 7). Therefore, if the maximum value of $I_{in,u}/K_i$ (0.15) is used in the evaluation of the inhibition of this pathway, the ciprofloxacin-induced increase in the $AUC_{po}$ of caffeine can be predicted as follows:

$$AUC_{po}(+\text{inhibitor})/AUC_{po}(\text{control}) = 1/\{f_h \cdot f_m/(1 + I_u/K_i) + (1 - f_h \cdot f_m)\} = 1.1$$

A 1.6-fold increase was actually observed, which indicates a greater degree of inhibition than predicted. Possible reasons for this discrepancy include the estimation error of $K_i$, the possibility that other metabolic pathways may also be inhibited by ciprofloxacin, and the accumulation of ciprofloxacin in the liver because of active transport. Indeed, we have recently demonstrated that a new quinolone antibiotic, grepafloxacin, is actively taken up by the rat liver (Sasabe *et al.,* 1997).

c. CYCLOSPORIN-ERYTHROMYCIN. Vereerstraeten *et al.* (1987) reported that the $AUC_{po}$ of cyclosporin (dose: 6 mg) increased about 1.6-fold after coadministration of 1.1 g erythromycin (table 8). Cyclosporin has many metabolic pathways, among which the metabolism to M1, M17, and M21 are mediated by CYP3A4 (Lensmeyer *et al.,* 1988). These metabolites are sequentially metabolized to form carboxylates in vivo (Pichard *et al.,* 1990). Because erythromycin is a specific inhibitor of CYP3A4, metabolic inhibition should be involved in this increase in the $AUC_{po}$ of cyclosporin. The $K_i$ of erythromycin for cyclosporin hydroxylation in human liver microsomes in vitro is about 75 $\mu$M (Miller *et al.,* 1990). The $I_{max}$ of erythromycin after a 1.1 g dose is 10–12 $\mu$M (Vereerstraeten *et al.,* 1987), and the absorption term [the second term in equation (22)] was calculated to be 15–93 $\mu$M using $k_a = 0.02–0.10\ min^{-1}$, D = 1.1 g, $Q_h$ = 1610 ml/min, and $F_a$ = 0.58. In the calculation of $k_a$ using $k_{el}(=0.693/t_{1/2})$ and $T_{max}$ (Lensmeyer *et al.,* 1988) based on equation (23), the maximum and minimum values were obtained taking the interindividual variation in $T_{max}$ into consideration. As mentioned above (see Section III.D.2.), however, it would be preferable to use the maximum value of $k_a$ in order to avoid a false negative prediction of the possibility of a drug-drug interaction. Equation (22) gives an $I_{in,max}$ of 25–105 $\mu$M. Because the $f_u$ of erythromycin is 0.16, $I_{in,u}$ and $I_{in,u}/K_i$ are calculated to be 4–17 $\mu$M and 0.05–0.23, respectively (table 8). The contribution of these metabolic pathways of cyclosporin to the total elimination ($CL_{oral}=f_b \cdot CL_{int}$) is about 76% ($f_h \cdot f_m = CL_{h,m}/CL_{tot} = 0.76$) (table 8). Therefore, if the maximum value of $I_{in,u}/K_i$ (0.23) is used in the evaluation of the inhibition of these pathways, the erythromycin-induced increase in the $AUC_{po}$ of cyclosporin can be predicted from equation (14) as follows:

$$AUC_{po}(+\text{inhibitor})/AUC_{po}(\text{control}) = 1/\{f_h \cdot f_m/(1 + I_u/K_i) + (1 - f_h \cdot f_m)\} = 1.2$$

This value is smaller than the observed 1.6-fold increase in $AUC_{po}$.

As mentioned above (see Section III.B.), however, the inhibition by erythromycin may not be due only to a competitive inhibition mechanism. Its demethylated metabolite is known to inactivate P450 by forming a complex with this enzyme (Periti *et al.,* 1992). Therefore, it may be inappropriate to estimate the pharmacokinetic alteration based only on the same methodology used for competitive inhibitors. Another methodology has to be developed for the prediction of in vivo drug-drug inter-

TABLE 8
*Inhibition of cyclosporin metabolism (CYP3A4) by coadministration of erythromycin*

| | Dose (mg) | Route | AUC (ng · hr/ml) | $CL_{tot}$ (ml/min/kg) | |
|---|---|---|---|---|---|
| control | 6 | p.o. | 9720 | 3.90 | |
| + erythromycin | | | 15200 | | |
| | $CL_r$ (ml/min/kg) | $CL_h$ (ml/min/kg) | $CL_{h,m}$ [a] (ml/min/kg) | $CL_{h,m}/CL_{tot}$ | $I_{in,u}/K_i$ |
| | 0.23 | 3.67 | 2.97 | 0.76 | 0.05–0.26 |

[a] formation of M1, M17 and M21.

actions based on the so-called "mechanism-based inhibition" of P450 from in vitro data; it should include the possible effects of inhibitor exposure time and the turnover of the enzyme, as will be discussed later in details (see Section III.G.).

Table 9 summarizes the results of the prediction of drug-drug interactions based on in vitro data. In some cases, in vivo pharmacokinetic parameters ($C_{max}$, AUC) were changed to some extent by drug-drug interactions although the values of $I_u/K_i$ calculated from in vitro data were too small to expect any metabolic inhibition in vivo. This finding suggests that alterations in in vivo pharmacokinetic parameters may be caused by other factors such as interactions involving absorption or excretion. Furthermore, in the case of macrolide antibiotics such as erythromycin, the model describing "the mechanism-based inhibition" should be introduced to predict the drug-drug interaction.

In order to avoid false negative predictions, one should not limit an interaction to a particular metabolic pathway, especially when the ratio of the pathway in question to the total clearance ($f_h \cdot f_m = CL_{h,m}/CL_{tot}$) is small, as in the cases with the terfenadine-ketoconazole interactions. The most important factor in the prediction is the accurate estimation of $I_u/K_i$. In other words, if the calculated value of $I_u/K_i$ for a particular metabolic pathway is high, the possible occurrence of drug interaction in vivo should be suspected, because it is likely that this inhibitor also inhibits another metabolic pathway(s) which has not been identified yet.

### *F. Procedure for Predicting Inhibitory Effects of Coadministered Drugs on the Hepatic Metabolism of Other Drugs*

The following is a proposed procedure for predicting the metabolic inhibition by one drug that is expected to be coadministered with the study drug being developed.

1) Confirmation of the involvement of P450 by in vitro inhibition studies, e.g., using SKF-525A and CO.
2) Identification of the P450 isozyme by metabolic studies using human P450 expression systems and the inhibition studies using P450 antibodies or inhibitors specific for each isozyme.
3) Searching the in vivo pharmacokinetic data for the coadministered drug that possibly inhibits the P450 isozyme catalyzing the metabolism of the drug under investigation. The maximum plasma unbound concentration of the coadministered inhibitor ($I_{in,max,u}$) can be estimated by $I_{max}$ (or $I_{max,ss}$), $k_a$ (or $T_{max}$ and $t_{1/2}$), $F_a$, and $f_u$ as described by equation (22).
4) Evaluation of the unbound concentration of inhibitor in the liver, which may be larger than $I_{in,max,u}$ in the case of an inhibitor that is actively transported into hepatocytes (fig. 3). The unbound concentration ratio (liver/plasma) should be measured by the method given below (see Section III.H.1.) using human hepatocytes (or rat isolated hepatocytes if human samples are not available). A 5- to 10-fold safety margin may also be considered for the concentration ratio if there are no experimental results available.
5) In vitro measurement of the $K_i$ of the inhibitor for the metabolism of the study drug using human liver microsomes or human P450 expression systems.
6) Assessing the possibility of metabolic inhibition by comparing the values of $I_{in,max,u}$ and $K_i$. If the $I_{in,max,u}/K_i$ value is larger than 0.3–1, you may want to consider designing the in vivo drug interaction studies. The limit of $I_{in,max,u}/K_i$ value should depend on the pharmacodynamic and/or toxicodynamic features and the therapeutic window of the drug investigated.

TABLE 9
*Summary of the prediction of in vivo drug-drug interaction from in vitro data based on competitive or noncompetitive inhibition mechanism*[a]

| | Inhibitor—Inhibited drug | AUC ratio[b] (Predicted AUC ratio[c]) | $I_{in,u}/K_i$[d] |
|---|---|---|---|
| (1) Successful cases: | (i) Sulfaphenazole—tolbutamide (2C9) | ×5.3 (×5.0) | 200 |
| | (ii) Ketoconazole—triazolam (3A4) | ×8.3 (×7.8) | 15 (α-OH), 4 (4-OH) |
| (2) Successful for the metabolic pathway but unsuccessful for the total: | (iii) Quinidine—sparteine (2D6) | ×2.9 (×1.3) | 60 |
| | (iv) Ketoconazole—terfenadine (3A4) | ×10 (×1.3) | 4 |
| (3) Unsuccessful for the metabolic pathway: | (v) Fluoxetine—imipramine (2D6) | ×1.9 (×1.0) | 0.07 |
| | (vi) Ciprofloxacin—caffeine (1A2) | ×1.6 (×1.1) | 0.15 |
| | (vii) Omeprazole—diazepam (2C19) | ×2.0 (×1.0) | 0.03 |
| | (viii) Erythromycin—triazolam (3A4) | ×2.1 (×1.0) | 0.017 (α-OH), 0.005 (4-OH) |

[a] Predictions were based on the inhibition of the P450 isozyme which is mainly related to the metabolism of the corresponding drug.
[b] Change in AUC induced by the drug-drug interaction (observed value).
[c] Change in AUC induced by the drug-drug interaction (predicted value).
[d] Index for the extent of the drug-drug interaction. $I_{in,u}$ was calculated using pharmacokinetic parameters of the drug.

Although a more precise and quantitative prediction requires the collection of more information and/or elaborate experiments, the authors think that the judgment of "absence of a metabolic drug-drug interaction" may be reliable if the interaction is not expected by this prediction method. The above metodology has been proposed based on the idea of avoiding false negative predictions. Therefore, it should be kept in mind that some of the predicted drug-drug interactions may not take place in vivo. We speculate that more than 80 combinations could be judged as "non-interacting" if 100 kinds of drug-drug interactions are investigated, at random, by this methodology. Of the less than 20 combinations involving possible interactions, cautious investigations using human in vivo studies would be necessary for some combinations, taking the therapeutic range, pharmacokinetic/pharmacodynamic characteristics, and severity of the adverse effects into consideration.

### G. Mechanism-Based Inhibition

*1. Characteristics of Mechanism-Based Inhibition.* In 1993, 15 Japanese patients with cancer and herpes zoster died from 5-fluorouracil (5-FU) toxicity caused by high blood concentrations caused by an interaction between 5-FU and sorivudine, an antiviral drug (Pharmaceutical Affairs Bureau, 1994). The interaction between sorivudine and 5-FU is based on "mechanism-based inhibition", which differs from the competitive or noncompetitive inhibition described so far (Desgranges *et al.,* 1986; Okuda *et al.,* 1997). A mechanism-based inhibitor is metabolized by an enzyme to form a metabolite which covalently binds to the same enzyme, leading to irreversible inactivation of the enzyme. Several terms such as "mechanism-based inactivation," "enzyme-activated irreversible inhibition," "suicide inactivation," and "$k_{cat}$ inhibition" have all been used as alternatives to "mechanism-based inhibition" (Silverman, 1988). It should be noted, however, that the inhibition is not called "mechanism-based inhibition" when the inhibitor is metabolically activated by an enzyme and inactivates another. Sorivudine is converted by gut flora to 5-bromovinyluracil (BVU), which is metabolically activated by dihydropyrimidine dehydrogenase (DPD), a rate-limiting enzyme in the metabolism of 5-FU (fig. 8) (Okuda *et al.,* 1995). Then, the activated BVU irreversibly binds to DPD itself. This type of interaction needs more attention than the common type of inhibition, because the inhibitory effect remains after elimination of the inhibitor (sorivudine, BVU) from blood and tissue and this can lead to serious side-effects.

Many drugs other than sorivudine also are reported to be mechanism-based inhibitors, including macrolide antibiotics such as erythromycin and troleandomycin (against CYP3A4) (Periti *et al.,* 1992), furafylline (against CYP1A2) (Kunze and Trager, 1993), and orphenadrine (against CYP2B1) (Murray and Reidy, 1990).

*2. Kinetic Analysis of Mechanism-Based Inhibition: Analysis of In Vitro Data.* Is it also possible to predict the extent of in vivo interactions from in vitro data in the case of mechanism-based inhibition? The first step in making such predictions is to construct a model describing the inhibition. Waley (1985) proposed the model shown in figure 9 for mechanism-based inhibition. Mass-balance equations for the enzyme-inhibitor complexes (EI and EI′) and the inactive enzyme ($E_{inact}$) can be expressed as follows:

$$d(EI)/dt = k_{+1} \cdot [I] \cdot E - (k_{-1} + k_2) \cdot EI \quad [25]$$

$$d(EI')/dt = k_2 \cdot EI - (k_3 + k_4) \cdot EI' \quad [26]$$

$$dE_{inact}/dt = k_4 \cdot EI' \quad [27]$$

where E and [I] represent the concentration of the active enzyme and the mechanism-based inhibitor, respectively. Because the total concentration of the enzyme ($E_o$) is maintained at a constant level,

$$E_o = E + EI + EI' \quad [28]$$

Combining equations (25), (26), and (28) yields the following equation, assuming a steady-state for EI and EI′ (i.e., d(EI)/dt = 0 and d(EI′)/dt = 0):

$$EI' = k_{+1} \cdot k_2 \cdot [I] \cdot E_o/((k_{+1} \cdot k_2 + k_{+1}(k_3 + k_4)) \cdot [I] + (k_3 + k_4)(k_{-1} + k_2)) \quad [29]$$

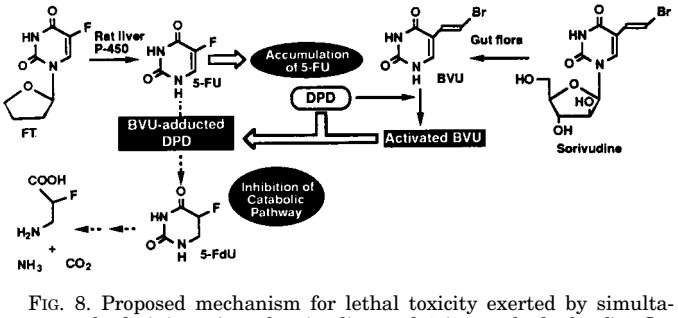


FIG. 8. Proposed mechanism for lethal toxicity exerted by simultaneous oral administration of sorivudine and 1-(2-tetrahydrofuryl)-5-fluorouracil (FT), a prodrug of 5-FU (Okuda *et al.,* 1995).

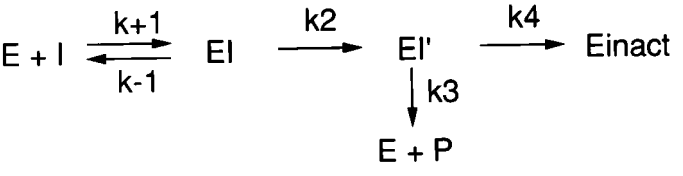


FIG. 9. Enzyme inhibition by a mechanism-based inhibitor (Waley 1985). E and $E_{inact}$ represent the active and inactive enzyme, respectively; I represents the mechanism-based inhibitor; EI and EI′ represent the enzyme-inhibitor complex I and II, respectively; and P represents the product.

Therefore, the initial inactivation rate of the enzyme under steady-state conditions ($V_{inact} = dE_{inact}/dt$) can be expressed as follows using equations (27) and (29):

$$\begin{aligned} V_{inact} &= k_{+1} \cdot k_2 \cdot k_4 \cdot [I] \cdot E_o/((k_{+1} \cdot k_2 + k_{+1}(k_3 + k_4)) \\ &\quad \cdot [I] + (k_3 + k_4)(k_{-1} + k_2)) \\ &= (k_2 \cdot k_4/(k_2 + k_3 + k_4) \cdot [I] \cdot E_o)/((k_3 + k_4)/(k_2 \\ &\quad + k_3 + k_4) \cdot (k_{-1} + k_2)/k_{+1} + [I]) \end{aligned} \quad [30]$$

As the initial inactivation rate of the enzyme at steady-state is equal to the initial decreasing rate of the active enzyme,

$$V_{inact} = -dE/dt(t = 0) = k_{obs} \cdot E(t = 0) = k_{obs} \cdot E_o \quad [31]$$

where $k_{obs}$ represents the apparent inactivation rate constant of the enzyme. The following equation can be derived from equations (30) and (31):

$$k_{obs} = V_{inact}/E_o = k_{inact} \cdot [I]_o/(K_{i,app} + [I]_o) \quad [32]$$

where

$$k_{inact} = k_2 \cdot k_4/(k_2 + k_3 + k_4) \quad [33]$$

$$K_{i,app} = (k_3 + k_4)/(k_2 + k_3 + k_4) \cdot (k_{-1} + k_2)/k_{+1} \quad [34]$$

Parameters ($k_{inact}$, $K_{i,app}$) required for predicting this model can be determined by in vitro studies as follows (fig. 10):

⟨1⟩ Preincubate the enzyme suspension for an appropriate period in the presence of various concentrations of inhibitor.
⟨2⟩ Mix the substrate solution with the enzyme suspension to measure the initial metabolic rate of the substrate so that the remaining enzymatic activity can be determined. The incubation time for this measurement should be as short as possible (around 1–3 min) compared with the preincubation time, in order to minimize the reaction of the inhibitor with the enzyme during the incubation.
⟨3⟩ Plot the logarithm of the enzymatic activity against the preincubation time. The apparent inactivation rate constant ($k_{obs}$) can be determined from the slope of the initial linear phase.
⟨4⟩ Obtain the parameters ($k_{inact}$, $K_{i,app}$) from the relationship between $k_{obs}$ and the initial inhibitor concentration ($[I]_o$) using the nonlinear least squares regression method.

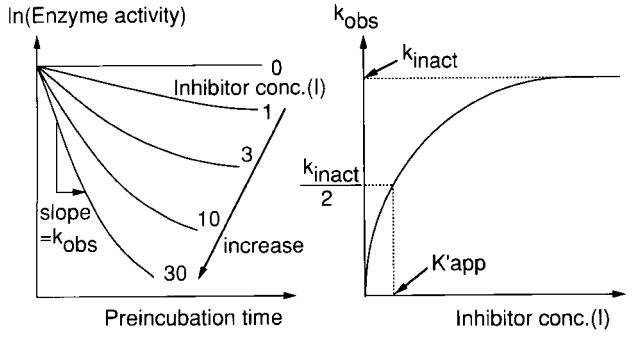


FIG. 10. Method to obtain kinetic parameters in vitro for mechanism-based inhibition.

Table 10 summarizes the results of the analysis of various combinations of P450 isozymes and mechanism-based inhibitors (Chiba *et al.,* 1995). The "partition ratio" in table 10 is defined as $k_3/k_4$ and can be obtained as the ratio of the amount of the inhibitor released as the product and the amount covalently bound to the enzyme. The larger the contribution of this inactivation pathway to the total elimination of the inhibitor in the in vitro system, the smaller the partition ratio. The partition ratio of the most powerful mechanism-based inhibitor is zero (every turnover produces inactivated enzyme).

It is clear from this model analysis that, in the case of mechanism-based inhibition, the inhibitor is metabolically activated by an enzyme and irreversibly inactivates the same enzyme by covalent binding, exhibiting the following characteristics:

a. Preincubation time-dependent inhibition of the enzyme (time-dependence).
b. No inhibition if cofactors necessary for producing the activated inhibitor (eg., NADPH for P450 metabolism) are not present in the preincubation medium.
c. Potentiation of the inhibition depending on the inhibitor concentration (saturation kinetics).
d. Slower inactivation rate of the enzyme in the presence of substrate compared with its absence (substrate protection).
e. Enzyme activity not recovered following gel filtration or dialysis (irreversibility).
f. 1:1 Stoichiometry of the inhibitor and the active site of the enzyme (stoichiometry of inactivation).

Mechanism-based inhibitors should satisfy these criteria.

*3. Prediction of In Vivo Interactions from In Vitro Data in the Case of Mechanism-Based Inhibition.* How can inhibitory effects in vivo be estimated from the microscopic inhibition parameters obtained from in vitro studies?

A simulation study was carried out using the perfusion model in figure 11 and the pharmacokinetic parameters in table 11. The inhibitor is assumed to inactivate a certain CYP isozyme in the liver in a "mechanism-based" manner. The differential equations for the substrate (S) and inhibitor (I) can be expressed as follows:

TABLE 10
*Comparison of inactivation parameters for mechanism-based P450 inactivators (Chiba* et al., *1995)*

| Inactivator | Target P450 | Assay Method (Source) | $k_{inact}$ ($min^{-1}$) | $K_{i,app}$ ($\mu M$) | Partition Ratio |
|---|---|---|---|---|---|
| L-754,394 | 3A4 | Testosterone 6$\beta$-hydroxylation (human liver microsomes) | 1.62 | 7.5 | 1.35 |
| Furafylline | 1A2 | (R)-warfarin 6-hydroxylation (human liver microsomes) | 0.87 | 23 | 3–6 |
| Gestodene | 3A4 | Nifedipine oxidation (human liver microsomes) | 0.39 | 46 | 9.0 |
| 6$\beta$-Thiotestosterone | 3A1/2 | Testosterone 6$\beta$-hydroxylation (rat liver microsomes) | 0.37 | 34 | NA[a] |
| Tienilic acid | 2C9 | Tienilic acid 5-hydroxylation (recombinant CYP 2C9) | 0.22 | 4.3 | 11.6 |
| *N*-methylcarbazole | 2B4 | Reduced CO-binding P450 spectrum (purified CYP 2B4) | 0.21 | 23 | NA |
| L-754,394 | 2D6 | Bufuralol 1′-hydroxylation (human liver microsomes) | 0.18 | 32 | 40.1 |
| *N*-methylcarbazole | 2B1 | Reduced CO-binding P450 spectrum (purified CYP 2B1) | 0.14 | 5.2 | NA |

[a] NA, Not available.

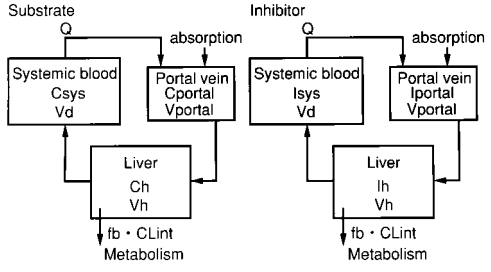


FIG. 11. Physiological model for the description of the time profiles of substrate and inhibitor concentrations in the plasma and liver. See the legend of Table 11 for the abbreviations used.

TABLE 11
*Parameters used in the simulation of mechanism-based inhibition*

| Substrate | Inhibitor |
|---|---|
| Dose = 2 $\mu$mol | Dose = 5000 $\mu$mol |
| $F_a$ = 0.8 | $F_a$ = 0.8 |
| $f_b$ = 0.1 | $f_b$ = 0.2 |
| $k_a$ = 0.01 $min^{-1}$ | $k_a$ = 0.02 $min^{-1}$ |
| $K_m$ = 100 $\mu$M | $K_m$ = 10 $\mu$M |
| $V_{max}(0)$ = 200 $\mu$mol/min | $V_{max}(0)$ = 30 $\mu$mol/min |
| $V_d$ = 70 L | $V_d$ = 20 L |
| $K_p$ = 1 | $K_p$ = 1 |
| Enzyme | Physiological parameters |
| $k_{deg}$ = 0.0005 $min^{-1}$ | Q = 1610 mL/min |
| $K_{i,app}$ = 20 $\mu$M | $V_h$ = 2800 mL |
| $k_{inact}$ = 0.06 $min^{-1}$ | $V_{portal}$ = 70 mL |
| $E_0$ = 5 nmol P450/g liver | |

Q, blood flow rate; $C_{sys}$ and $I_{sys}$, concentration in systemic blood; $V_d$, volume of distribution in the central compartment; $C_{portal}$ and $I_{portal}$, concentration in portal vein; $V_{portal}$, volume of portal vein; $C_h$ and $I_h$, concentration in liver; $V_h$, volume of liver; $f_b$, unbound fraction in blood; $CL_{int}$, intrinsic metabolic clearance; $F_a$, fraction absorbed from the intestinal tract; $K_m$, Michaelis constant for the metabolic elimination; $V_{max}$, Maximum metabolic rate for the metabolic elimination; $K_p$, liver-to-blood concentration ratio.

For S;

$$V_h \cdot (dC_h/dt) = Q \cdot C_{portal} - Q \cdot C_h/K_p - f_b \cdot CL_{int} \cdot C_h/K_p \quad [35]$$

$$CL_{int} = V_{max}/(K_m + f_b \cdot C_h/K_p) \quad [36]$$

$$V_{max} = V_{max}(0) \cdot E_{act}(t)/E_o \quad [37]$$

$$V_{portal} \cdot (dC_{portal}/dt) = Q \cdot C_{sys} + V_{abs} - Q \cdot C_{portal} \quad [38]$$

$$V_{abs} = k_a \cdot D \cdot F \cdot e^{-ka \cdot t} \quad [39]$$

$$V_d \cdot (dC_{sys}/dt) = Q \cdot C_h/K_p - Q \cdot C_{sys} \quad [40]$$

For I;

$$V_h \cdot (dI_h/dt) = Q \cdot I_{portal} - Q \cdot I_h/K_p - f_b \cdot CL_{int} \cdot I_h/K_p \quad [41]$$

$$CL_{int} = V_{max}/(K_m + f_b \cdot I_h/K_p) \quad [42]$$

$$V_{portal} \cdot (dI_{portal}/dt) = Q \cdot I_{sys} + V_{abs} - Q \cdot I_{portal} \quad [43]$$

$$V_{abs} = k_a \cdot D \cdot F \cdot e^{-ka \cdot t} \quad [44]$$

$$V_d \cdot (dI_{sys}/dt) = Q \cdot I_h/K_p - Q \cdot I_{sys} \quad [45]$$

where Q represents blood flow rate, $C_{sys}$ and $I_{sys}$ represent concentration in systemic blood, $V_d$ represents volume of distribution in the central compartment, $C_{portal}$ and $I_{portal}$ represent concentration in portal vein, $V_{portal}$ represents volume of portal vein, $C_h$ and $I_h$ represent concentration in the liver, $V_h$ represents volume of liver, $f_b$ represents unbound fraction in blood, $CL_{int}$ represents intrinsic metabolic clearance, $F_a$ represents fraction absorbed from the gastrointestinal tract, $K_m$ represents Michaelis constant for the metabolic elimination, $V_{max}$ represents maximum metabolic rate, and $K_p$ represents liver-to-blood concentration ratio.

The following assumptions were made in the mass-balance equations (35 to 45):

a. S and I are simultaneously administered orally.
b. Both S and I are eliminated only in the liver and their elimination can be described by the Michaelis-Menten equation.
c. Distribution of S and I in the liver rapidly reaches equilibrium, and the unbound concentration in the hepatic vein is equal to that in the liver at equilibrium (well-stirred model).
d. The unbound molecule in the liver is related to the elimination.
e. The contribution of the CYP isozyme subject to inactivation is small in total elimination of the inhibitor in the liver (i.e., the elimination of the inhibitor itself is not altered by inactivation of the enzyme).
f. Gastrointestinal absorption can be described by a first-order rate constant.

Furthermore, it should be noted that $V_{max}$ of the substrate is assumed to be proportional to the amount of active enzyme ($E_{act}$) in equation (37).

The differential equations for active and inactive enzyme in the liver ($E_{act}$ and $E_{inact}$, respectively) can be described as follows:

$$\frac{dE_{act}}{dt} = -\frac{k_{inact} \cdot E_{act} \cdot f_b \cdot I_h/K_p}{K_{i,app} + f_b \cdot I_h/K_p} + k_{deg}(E_o - E_{act}) \quad [46]$$

$$\frac{dE_{inact}}{dt} = \frac{k_{inact} \cdot E_{act} \cdot f_b \cdot I_h/K_p}{K_{i,app} + f_b \cdot I_h/K_p} - k_{deg} \cdot E_{inact} \quad [47]$$

where $k_{deg}$ represents the degradation rate constant (turnover rate constant) of the enzyme. The initial conditions (at $t = 0$) are $E_{act} = E_o$ and $E_{inact} = 0$. In the absence of an inhibitor, the enzyme level in the liver is at steady-state and the degradation rate ($k_{deg} \cdot E_o$) is equal to the synthesis rate, which is assumed to be unaffected by an inhibitor.

a. BASIC SIMULATION. Using the physiological model in figure 11 and the parameters in table 11, time courses of inhibitor blood concentrations, active enzyme levels in the liver ($E_{act}$), and substrate blood concentrations have been simulated with the dose of the inhibitor ranging from 0 to 50,000 $\mu$mol (fig. 12). The above eight differential equations (three for the substrate, three for the inhibitor, and two for the enzyme level in the liver) were numerically solved. The elimination rate of the active enzyme ($E_{act}$) increases with an increasing dose of the inhibitor, resulting in the prolonged elimination of the substrate.

b. EFFECT OF THE TURNOVER RATE OF THE ENZYME. The effect of the turnover rate constant of the enzyme ($k_{deg}$) on the profiles of $E_{act}$ and the substrate elimination were investigated in the simulation study. Basic parameters in table 11 were used except that $k_{deg}$ was changed to cover the range of 0.00005–0.005 $min^{-1}$. As the inhibitor itself is gradually eliminated from blood and liver, the enzyme level recovers to reach its initial level by replacement of the inactivated enzyme by newly synthesized enzyme (fig. 13). The faster the turnover rate of the enzyme, the faster the enzyme level is restored to its initial level.

c. TIMING OF INHIBITOR ADMINISTRATION. One of the characteristics of the mechanism-based inhibition is that the effect remains even after the inhibitor is eliminated from the body. Therefore, the inhibitory effect may depend on the timing of the substrate administration, even if the same dose of the inhibitor is administered. Simulations shown in figure 14 indicate that the most potent inhibitory effect can be obtained by having an appropriate interval between administration of the inhibitor and the substrate. Too short an interval will lead to completion of the kinetic event of the substrate before sufficient inactivation of the enzyme occurs, and too long an interval will allow the enzyme to recover. Both situations will result in a reduction of the inhibitory effect.

d. POSSIBILITY OF IN VITRO/IN VIVO SCALING. Figure 15 shows the effects of two parameters obtained in the in vitro studies ($k_{inact}$ and $K_{i,app}$) on the simulated in vivo profiles of $E_{act}$ and substrate blood concentrations. As expected, in vivo inactivation of the enzyme and prolongation of substrate elimination become marked with a larger $k_{inact}$ and a smaller $K_{i,app}$. In the future, it will be necessary to examine whether this method can properly predict in vivo effects from in vitro data. What kind of approach should be taken to verify this methodology? For example, although estimation of the unbound concentration of inhibitor in the liver is important for any prediction, it is impossible to measure this, especially in humans. Instead, kinetic parameters can be determined to fit the inhibitor blood concentration profile, which is measured in most cases. However, undetermined parameters, such as the liver-to-plasma concentration ra-

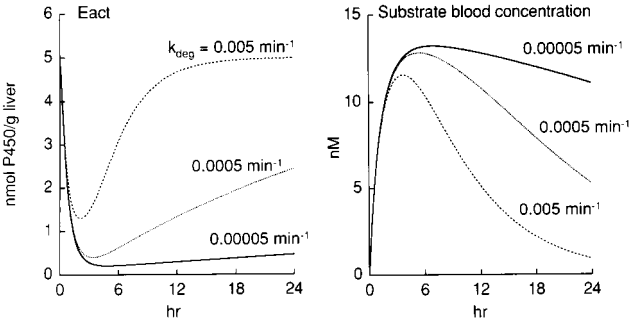


FIG. 13. Effects of turnover rate of the enzyme on the active enzyme level in the liver and substrate blood concentration.

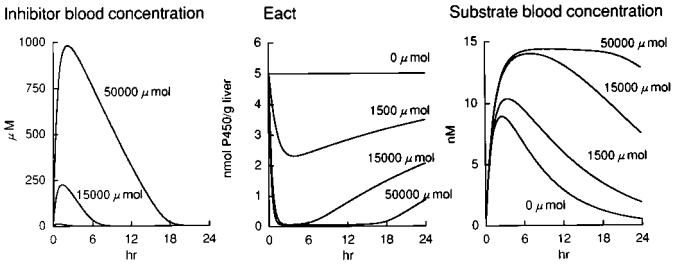


FIG. 12. Effects of the dose of inhibitor on inhibitor blood concentration, the active enzyme level in the liver and substrate blood concentration. The substrate and the inhibitor were assumed to be administered simultaneously.

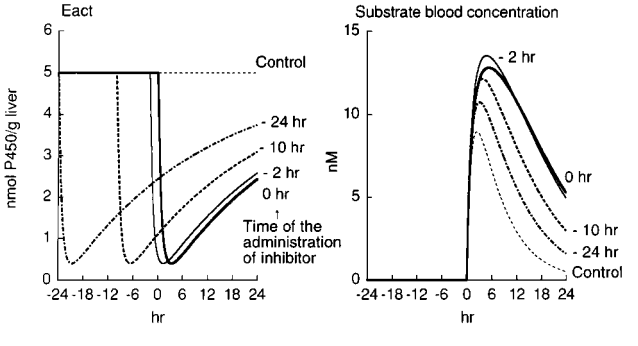


FIG. 14. Effects of administration interval of the inhibitor and substrate on the active enzyme level in the liver and substrate blood concentration.

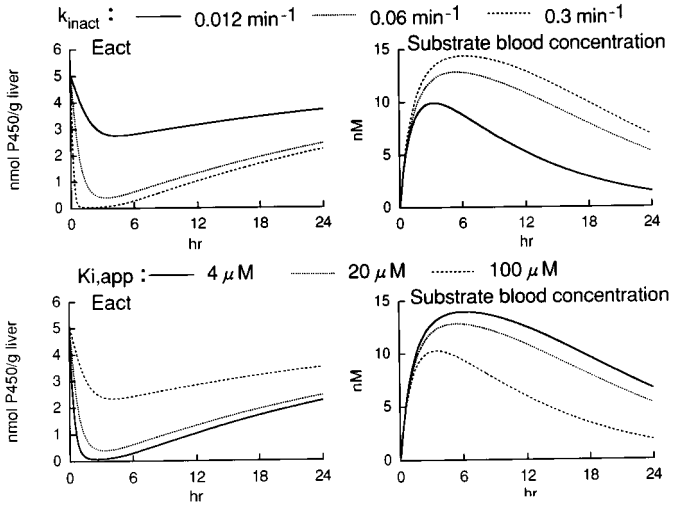


FIG. 15. Effects of $k_{inact}$ and $K_{i,app}$ on the active enzyme level in the liver and substrate blood concentration.

tio, need to be varied within certain limits in the simulation study so that the range of alteration in the profiles of $E_{act}$ and substrate can be predicted.

It is also important to confirm the validity of the prediction method in animal studies, where the inhibition studies can be performed both in vitro (using e.g. liver microsomes for P450) and in vivo. Because invasive experiments are possible in this case, including measurements of the distribution kinetics of the inhibitor in the liver, this may allow for more accurate predictions.

### *H. Problems To Be Solved for the More Precise Prediction of Drug-Drug Interactions*

*1. Estimation of the Tissue Unbound Concentration of the Inhibitor That Is Actively Transported into Hepatocytes.* As described above (see Section III.D.), in vivo drug-drug interactions based on inhibition of hepatic metabolism can be predicted by the values of $K_i$ and the unbound concentration of the inhibitor in the liver, which cannot be directly measured in vivo. The analyses have been based on the assumption that the steady-state unbound concentration of the inhibitor in the liver is equal to that in the hepatic capillary (sinusoid), because many drugs are transported into hepatocytes by passive diffusion. However, in the case of an inhibitor that is concentrated in hepatocytes by active transport (Yamazaki *et al.,* 1995, 1996), the extent of the interaction may be underestimated if plasma concentrations are used in the prediction.

Zomorodi and Houston (1995) investigated the effect of omeprazole on diazepam metabolism using rat liver microsomes and hepatocytes. Omeprazole inhibited both 3-hydroxylation and N-demethylation of diazepam, and the $K_i$ in hepatocytes was smaller than that in microsomes for both pathways (table 12). On the other hand, as shown in figure 16, the in vivo clearance of diazepam was reduced depending on omeprazole concentration,

TABLE 12
*Omeprazole inhibition of diazepam metabolism in hepatic microsomes and hepatocytes (Zomorodi and Houston, 1995)*

| | Pathway | |
|---|---|---|
| | 3HDZ | NDZ |
| Microsomal $K_i$ ($\mu$M)[a] | 108 ± 30 | 226 ± 76 |
| Hepatocyte $K_i$ ($\mu$M)[b] | 28 ± 11 | 59 ± 27 |
| Microsomal $K_m/K_i$ | 1.1 | 0.1 |
| Hepatocyte $K_m/K_i$ | 2.5 | 0.6 |

[a] Mean ± SD, n = 4.
[b] Mean ± SD, n = 3.

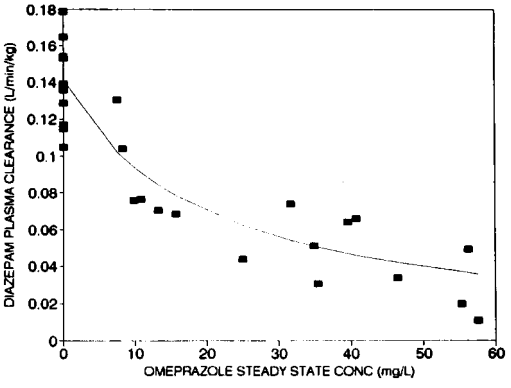


FIG. 16. Relationship between diazepam clearance and steady-state concentration of omeprazole in rats (Zomorodi and Houston, 1995).

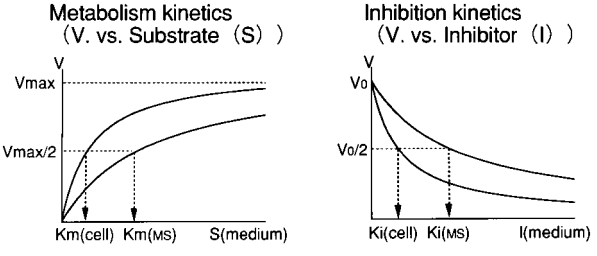


FIG. 17. The difference in $K_m$ or $K_i$ values obtained in the metabolism studies using hepatocytes (Cell) and microsomes (MS) in the case of a drug which is actively transported into the liver. V represents the initial velocity of the metabolite formation.

which was maintained under steady-state conditions. In this in vivo study, the $K_i$ was calculated to be 57 $\mu$M from equation (48).

$$CL = CL_o/(1 + I_{ss}/K_i) \quad [48]$$

where $CL_o$ represents diazepam clearance in the absence of omeprazole, and $I_{ss}$ represents the steady-state total plasma concentration of omeprazole. The in vivo $K_i$ showed closer agreement with the $K_i$ values obtained in hepatocytes than with those observed in microsomes (table 12). Their results, however, should be interpreted cautiously, because the $K_i$ was calculated based on the amount of drug added to the medium instead of the unbound concentration, and the total plasma concentration in vivo was used as the $I_{ss}$ in equation (48) instead of the unbound concentration, which should be related to the metabolic inhibition. As shown in figure 17, $K_m$ or $K_i$

values obtained in the metabolism studies based on the medium concentration of substrates and inhibitors, respectively, may be smaller in hepatocytes than in microsomes if the molecule is actively transported into hepatocytes. The difference is reflected in the cell-to-medium unbound concentration ratio (C/M ratio) as shown in equation (49):

$$\text{C/M ratio} = K_m(\text{MS})/K_m(\text{Cell}) = K_i(\text{MS})/K_i(\text{Cell}) \quad [49]$$

where MS and Cell in parentheses indicate the values obtained in microsomes and in cells, respectively. Therefore, the difference in the $K_i$ values of omeprazole obtained in liver microsomes and hepatocytes may be explained by the accumulation of omeprazole in hepatocytes by active transport.

The active transport of drugs can be evaluated by measuring the drug uptake into hepatocytes or liver slices in the presence and absence of adenosine triphosphate (ATP)-depletors such as rotenone and FCCP (Yamazaki *et al.,* 1993; Nakamura *et al.,* 1994). Assuming both active transport and passive diffusion for the influx into hepatocytes and only passive diffusion for the efflux from the hepatocytes (figure 18), the initial uptake velocity in the presence of an adequate concentration of ATP-depletor represents the uptake by passive diffusion, because the active transport of the drug is completely inhibited. C/M ratio in the steady-state can be described by equation (50):

$$\text{C/M ratio} = (PS_{active} + PS_{passive})/PS_{passive} = v_o/v_{passive} \quad [50]$$

where $PS_{active}$ and $PS_{passive}$ represent the membrane permeation clearance by active transport and passive diffusion, respectively; $v_o$ and $v_{passive}$ represent the initial uptake velocity obtained in the absence and presence of ATP-depletors, respectively. This C/M ratio can also be calculated by measuring the steady-state drug concentration (sum of the bound and unbound forms) in the cell and that in the medium in the absence and presence of the ATP-depletor as follows:

$$\frac{C_{cell}/C_{medium}(\text{control})}{C_{cell}/C_{medium}(+\text{ ATP-depletor})} = \frac{C_{cell,free}/f_T/C_{medium}(\text{control})}{C_{cell,free}/f_T/C_{medium}(+\text{ ATP-depletor})} = \frac{C_{cell,free}(\text{control})}{C_{medium}} = \text{C/M ratio} \quad [51]$$

where $C_{cell}$ and $C_{medium}$ represent steady-state total drug concentration in the cell and that in the medium, respectively; $C_{cell,free}$ represents steady-state unbound drug concentration in the cell; and $f_T$ represents the unbound fraction in the cell. It is assumed that $f_T$ is not affected by the ATP-depletor and that $C_{cell,free}$ equals $C_{medium}$ in the presence of the ATP-depletor. Equation (51) can be used even when active transport is involved in the efflux process out of the hepatocytes, whereas equation (50) cannot be applied in such a case.

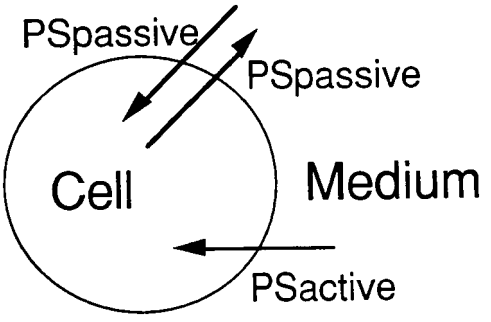


FIG. 18. A model for drug transport into and out of the hepatocyte. $PS_{active}$ and $PS_{passive}$ represent the membrane permeation clearance by active transport and passive diffusion, respectively.

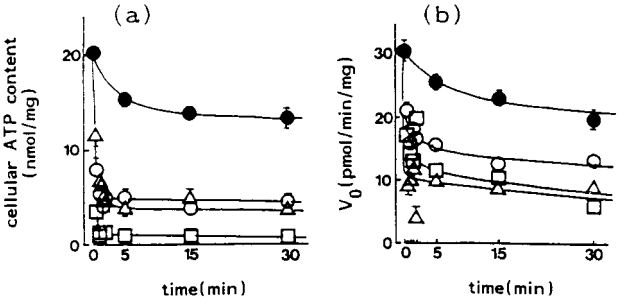


FIG. 19. Effect of ATP depletors on cellular ATP content (a) and the initial uptake velocity ($V_o$) of [$^3$H]cimetidine into hepatocytes (b) (Nakamura *et al.,* 1994). ●: control; □: with FCCP (2 $\mu$M); △: with rotenone (30 $\mu$M); ○: with sodium azide (30 mM).

Nakamura *et al.* (1994) reported that FCCP, rotenone, or sodium azide causes a marked reduction in the uptake of [$^3$H]cimetidine into isolated rat hepatocytes that parallel the reduction in cellular ATP (fig. 19). The unbound concentration ratio of cimetidine in hepatocytes in this case can be calculated to be about 5.6 according to equation (50). If the unbound concentration ratio in a linear condition ($C_{medium} \ll K_m$) is calculated from equations (50) and (52) using the values of $V_{max}$, $K_m$, and $PS_{passive}$ which were determined by fitting the initial uptake velocity ($v_o$) to equation (53), a value of 7.1 can be obtained:

$$PS_{active} = V_{max}/(K_m + C_{medium}) \quad [52]$$

$$v_o = V_{max}C_{medium}/(K_m + C_{medium}) + PS_{passive}C_{medium} \quad [53]$$

Here, in this calculation, it is assumed that carrier-mediated saturable uptake represents active transport. The $K_i$ value of cimetidine for the metabolism of ethoxyresorufin and those values for $\alpha$-hydroxylation and 4-hydroxylation of triazolam in human liver microsomes are 600 $\mu$M, 36 $\mu$M, and 160 $\mu$M, respectively (Knodell *et al.,* 1991; Von Moltke *et al.,* 1996). The unbound concentration ratios (liver/plasma) when the intracellular unbound concentration is 600 $\mu$M, 160 $\mu$M, and 36 $\mu$M are calculated to be about 1.5, 3.7, and 6.4, respectively, using the parameters for carrier-mediated transport reported by Nakamura *et al.* (1994). This cal-

culation indicates that the lower the plasma concentration of inhibitor, the higher the liver-to-plasma unbound concentration ratio, when the carrier-mediated active transport (influx) is operating.

We previously reported (Yamazaki *et al.,* 1993) that concentration of pravastatin, an HMG-CoA reductase inhibitor, in isolated rat hepatocytes was about 3- to 7-fold higher than that in medium because of active transport. It was also suggested that simvastatin and lovastatin, which competitively inhibited the hepatic uptake of pravastatin, may be transported by the same carrier as pravastatin (Yamazaki *et al.,* 1993). Since the HMG-CoA reductase inhibitors such as fluvastatin, simvastatin, and pravastatin inhibit CYP2C9-mediated 4′-hydroxylation of diclofenac (Transon *et al.,* 1996), the concentrative uptake into hepatocytes should be taken into consideration in predicting interactions involving these drugs.

In the future, more accurate predictions of in vivo drug-drug interactions may become possible by estimating the unbound concentration of the inhibitor in the liver in in vitro studies.

*2. Evaluation of Drug-Drug Interactions Involving Drug Metabolism in the Gut.* CYP3A4, an enzyme that metabolizes many drugs, including cyclosporin, exists not only in the liver but also in the gut; it plays an important role in the first-pass metabolism after oral administration of its substrates (Kolars *et al.,* 1991, 1992; Thummel *et al.,* 1996). De Waziers *et al.* (1990) have used Western blot analysis and shown that CYP3A4 is highly expressed in the duodenum and jejunum, secondly to the liver, in humans (fig. 20).

As shown in figure 21, the bioavailability (BA) of cyclosporin after oral administration was reduced by coadministration of rifampicin, an inducer of CYP3A4, and increased by coadministration of ketoconazole or erythromycin, which are inhibitors of CYP3A4 (Hebert *et al.,* 1992; Gomez *et al.,* 1995; Gupta *et al.,* 1989). Wu *et al.* (1995) attempted to differentiate the absorption and first-pass gut and hepatic metabolism of cyclosporin in humans by a kinetic analysis of the change in BA by rifampicin-induced induction and ketoconazole- or erythromycin-induced inhibition of CYP3A4-mediated metabolism. Based on the model shown in figure 22, BA after oral administration can be expressed as follows using the fraction of the drug dose absorbed into and through the gastrointestinal membranes ($F_{abs}$), the fraction of the absorbed dose that passes through the gut into the hepatic portal blood unmetabolized ($F_g$), and the hepatic first-pass availability ($F_h$):

$$\begin{aligned} BA &= F_{abs}F_gF_h \\ &= F_{abs}(1 - E_g)(1 - E_h) \end{aligned} \quad [54]$$

where $E_g$ and $E_h$ represent gut and hepatic extraction ratio, respectively. Assuming that $F_{abs}$ is not altered by the enzyme inducer or the inhibitor, BA after coadmin-

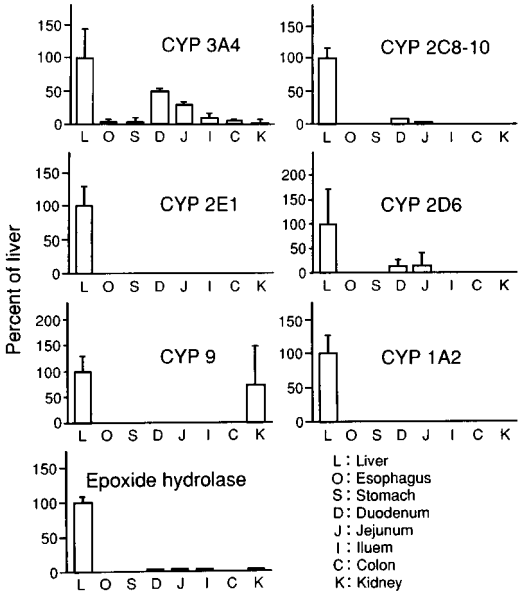


FIG. 20. Immunoquantification of P450s and epoxide hydrolase in human liver and extrahepatic microsomes using Western blots (De Waziers *et al.,* 1990).

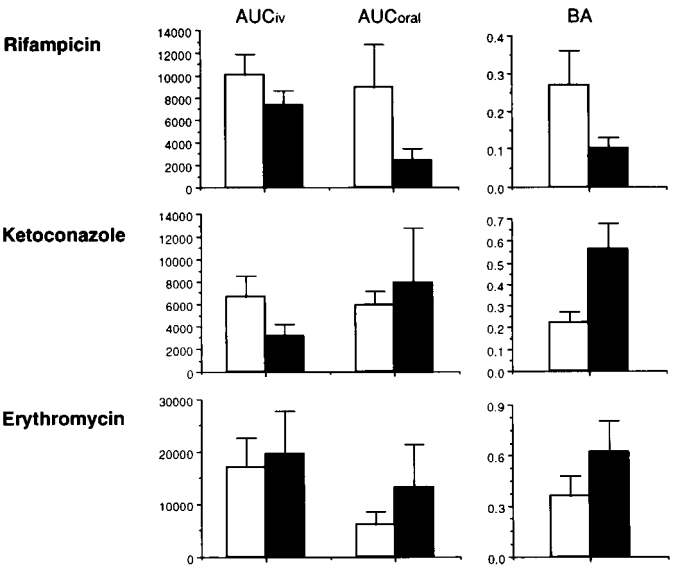


FIG. 21. Effects of rifampicin, ketoconazole, and erythromycin on the disposition of cyclosporin (Hebert *et al.,* 1992; Gomez *et al.,* 1995; Gupta *et al.,* 1989). Open column: control; Closed column: with the interacting drug.

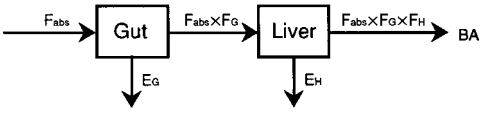


FIG. 22. Schematic diagram depicting the effects of absorption and gut and hepatic first-pass extraction on drug oral bioavailability (Wu *et al.,* 1995). $F_{abs}$: Fraction of the drug dose absorbed into and through the gastrointestinal membranes; $F_G$: fraction of the absorbed dose that passes through the gut into the hepatic portal blood unmetabolized; $F_H$: the hepatic first-pass availability; BA: oral bioavailability; $E_G$ and $E_H$: gut and hepatic extraction ratio, respectively.

istration of the interacting drug can be expressed as follows:

$$BA = F_{abs}(1 - X_g E_g)(1 - X_h E_h) \quad [55]$$

where $X_g$ and $X_h$ represent the changes in the gut and hepatic extraction ratio, respectively, during coadministration of the interacting drug. Assuming that the drug is eliminated only by the liver and kidney, as is the case for many drugs, $E_h$ can be calculated by the following equation:

$$E_h = CL_h/Q_h = (CL_{tot} - CL_r)/Q_h \quad [56]$$

where $CL_{tot}$ can be estimated from the dose divided by the AUC after intravenous administration and $CL_r$ can be estimated by multiplying $CL_{tot}$ and the urinary excretion rate of the parent compound. Furthermore, $X_h$ in equation (55) can be obtained as the ratio of $E_h$ in the presence and absence of the interacting drug. Equations (54) and (55) then contain three unknown parameters ($F_{abs}$, $E_g$, and $X_g$), allowing the calculation of $E_g$ and $X_g$ by fixing the value of $F_{abs}$. The maximum value of $F_{abs}$ was set at 1 (complete absorption), and the minimum value was calculated by dividing BA by $F_h$ ($=1 - E_h$) at the time when the metabolism was inhibited by the interacting drug (assuming $F_g = 1$). As shown in table 13, the calculated extraction ratio in the gut was always larger than that in the liver, irrespective of the value of $F_{abs}$. Furthermore, $X_g$ was larger than $X_h$ when $F_{abs}<86\%$ in the case of rifampicin coadministration and was smaller than $X_h$ in the case of erythromycin coadministration, indicating that the interaction observed in the gut is about the same or larger than that observed in the liver.

Therefore, the drug-drug interaction based on metabolic inhibition in the gut after oral administration cannot be neglected, especially for the drugs metabolized by CYP3A4. The methodology for the prediction of in vivo first-pass gut metabolism from in vitro studies using human gut samples needs to be established.

On the other hand, it is known that p-gp exists in the luminal membrane of gut epithelial cells and acts as an efflux transporter (Saitoh and Aungst, 1995; Terao *et al.,* 1996). Recent studies have revealed the overlapping substrate specificity of CYP3A4 and p-gp. As shown in table 14, many substrates of CYP3A4 are reported to be substrates or inhibitors of p-gp (Wacher *et al.,* 1995). In another study (Schuetz *et al.,* 1996) using a cell line derived from a human colon adenocarcinoma, it was shown that many of the p-gp inducers also induce CYP3A4, suggesting the possibility of common regulatory factors for these proteins (table 15).

Benet (1995, 1996) has pointed out the possibility that the synergistic effects of CYP3A4-mediated metabolism and p-gp-mediated efflux in the gut epithelium may result in an unexpectedly high first-pass effect in the gut after oral administration. Thus, the inhibition or induction of CYP3A4 and/or p-gp caused by drug-drug interactions may affect the first-pass effect in the gut.

The effects of gut metabolism and efflux from epithelial cells to the lumen on the absorption of orally administered drugs were investigated by a simulation study. Based on the compartment model shown in figure 23, the fraction of the drug absorbed into the portal vein ($F_a$) can be expressed as follows:

$$F_a = \frac{P_3}{CL_{int} + P_3}\left\{1 - \exp\left(-\alpha_1 \times \frac{CL_{int} + P_3}{P_2 + CL_{int} + P_3}\right)\right\} \quad [57]$$

where $P_2$, $P_3$, and $CL_{int}$ represent the clearance for efflux from the cell to the lumen, absorption from the cell to the portal vein, and intracellular metabolism, respectively, and $\alpha_1$ is the membrane permeation constant from the lumen into the cell. $\alpha_1$ is a hybrid parameter with no dimensions, consisting of the transit time in the lumen, diffusion in the unstirred water layer, and the permeability through the brush-border membrane of the gut epithelial cells:

$$\alpha_1 = \frac{P_{1,app} \times \overline{t_{gi}}}{V_{av}} \quad [58]$$

where $P_{1,app}$ represents the apparent influx clearance from the lumen into the cell, $\overline{t_{gi}}$ represents small intestinal transit time, and $V_{av}$ represents the average luminal volume.

The results are shown in figure 24. When $CL_{int}+P_3$ is much larger than $P_2$, equation (57) can be rearranged to yield equation (59):

$$F_a = \frac{P_3}{CL_{int} + P_3}\{1 - \exp(-\alpha_1)\} \quad [59]$$

In this case, $F_a$ is not affected by a change in $P_2$ possibly caused by inhibition of p-gp (fig. 24 left panel). If $CL_{int}$

TABLE 13
*Gut and hepatic extraction of cyclosporine and the effects of enzyme inducers and inhibitors at the boundary conditions for absorption (Wu* et al., *1995)*

| | $F_{abs}$ | $E_G$ | $X_G$ | $E_H$ | $X_H$ |
|---|---|---|---|---|---|
| Rifampicin | 100% | 0.65 | 1.31 | 0.33 | 1.40 |
| | 86% | 0.59 | 1.40 ($X_G = X_H$) | | |
| | 77% | 0.54 | 1.49 | | |
| | 65% | 0.46 | 1.68 | | |
| Ketoconazole | 100% | 0.71 | 0.49 | 0.14 | 0.56 |
| | 86% | 0.66 | 0.36 | | |
| | 77% | 0.62 | 0.25 | | |
| | 65% | 0.55 | Indeterminate | | |
| Erythromycin | 100% | 0.51 | 0.44 | 0.20 | 0.78 |
| | 86% | 0.43 | 0.23 | | |
| | 77% | 0.37 | Indeterminate | | |

$F_{abs}$, Fraction of the drug dose absorbed into and through the gastrointestinal membranes.

$E_G$, $E_H$, Gut and hepatic extraction ratio, respectively.

$X_G$, $X_H$, Changes in $E_G$ and $E_H$, respectively, during coadministration of the interacting drug.

TABLE 14
*Substrates for and inhibitors of both CYP3A and P-gp (Wacher* et al., *1995)*

| CYP3A substrates | P-gp | CYP3A substrates | P-gp | CYP3A substrates | P-gp |
|---|---|---|---|---|---|
| Antiarrhythmics | | Chemotherapeutic agents | | Hormones | |
| Amiodarone | I | Etoposide | S | Dexamethasone | S |
| Lidocaine | I | Doxorubicin | S[a] | Estradiol | S[b] |
| Quinidine | I | Paclitaxel | S | Hydrocortisone | S,I |
| Antifungals | | Vinblastine | S | Progesterone | I |
| Itraconazole | I | Vincristine | S | Testosterone | I |
| Ketoconazole | I | Vindesine | S | Others | |
| Flavonoids | | Ca-channel blockers | | Digitoxin | S[c] |
| Kaempferol (I) | E | Diltiazem | S,I | Erythromycin | I |
| Quercetin (I) | E | Felodipine | I | RU486 | I |
| Immunosuppressants | | Nicardipine | S,I | Tamoxifen | I |
| Cyclosporine | S,I | Nitrendipine | I | Terfenadine | I |
| FK506 | S,I | Nifedipine | I | | |
| Rapamycin | S | Verapamil | S,I | | |

S, Substrate; I, Inhibitor; E, Enhancer.
[a] Doxorubicin, a precursor of morpholino doxorubicin, is a P-gp substrate.
[b] 17-$\beta$ estradiol glucuronide, a phase II metabolite of estradiol, is a P-gp substrate.
[c] Digoxin, a metabolite of digitoxin, is a P-gp substrate.

TABLE 15
*Effect of various drugs on expression of P-glycoprotein and CYP3A in LS180 cells (Schuetz* et al., *1996)*

| Treatment | Fold-increase in Pgp | Rank order (Pgp) | Fold-increase in CYP3A4/5 | Rank order (CYP3A) |
|---|---|---|---|---|
| Reserpine | 29 ± 3.3[a] | 1 | 7.6 ± 0.6 | 1 |
| Rifampicin | 16.2 ± 10.8 (range, 6.2–29.9) | 2 | 3.2 ± 1.4 | 3 |
| Phenobarbital | 14.4 ± 3.6 (range, 6.0–22) | 3 | 6.1 ± 3.3 | 2 |
| Verapamil | 10.8 ± 8.3 | 4 | 1.7 ± 0.4 | 7 |
| Midazolam | 5.9 ± 1.7 | 5 | 1.0 | |
| Rapamycin | 4.9 ± 2.1 | 6 | 1.0 | |
| Clotrimazole | 4.1 ± 1.3 | 7 | 4.5 ± 1.1 | 5 |
| FK506 | 3.2 ± 0.7 | 8 | 1.3 ± 0.2 | 9 |
| Isosafrole | 2.7 ± 0.3 | 9 | 2.6 ± 0.1 | 6 |
| Amiodarone | 2.4 ± 0.7 | 10 | 1.0 | |
| Triacetyloleandomycin | 2.3 ± 0.8 | 11 | 1.5 ± 0.2 | 8 |
| Erythromycin | 2.0 ± 0.6 | 12 | 5.3 ± 1.2 | 4 |
| Dexamethasone | 1.5 ± 0.3 | 13 | 1.0 | |
| Nifedipine | 1.3 ± 0.1 | 14 | 1.0 | |
| Phenytoin | 1.3 ± 0.1 | 15 | 1.0 | |

[a] The values are the mean of up to five separate determinations ± standard deviations; values of 1.0 = no change from untreated control. All cultures were treated for 48–72 hr with 10 $\mu$M drug, except for phenobarbital (1 mM).

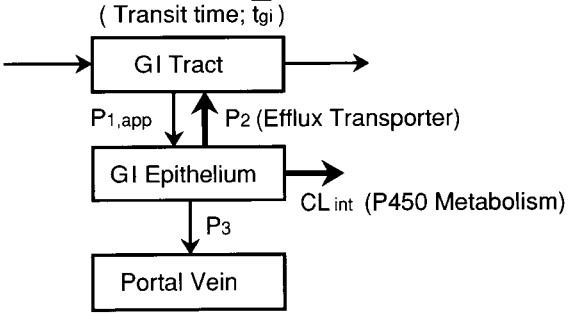


FIG. 23. A compartment model used in the simulation of the effects of gut metabolism and efflux to the lumen on the drug absorption. $P_{1,app}$: apparent influx clearance from the lumen into the cell; $P_2$: efflux clearance from the cell to the lumen; $P_3$: absorption clearance from the cell to the portal vein; $CL_{int}$: intracellular metabolic clearance.

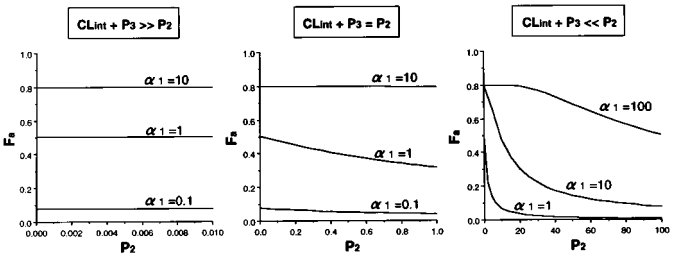


FIG. 24. Effect of the inhibition of efflux (reduction in $P_2$) on drug absorption. $F_a$: fraction of the drug absorbed into the portal vein; $\alpha_1$: membrane permeation constant from the lumen into the cell; $P_2$: efflux clearance from the cell to the lumen; $P_3$ (=0.8): absorption clearance from the cell to the portal vein; $CL_{int}$ (=0.2): intracellular metabolic clearance.

+ $P_3$ is much smaller than $P_2$, equation (60) can be derived:

$$F_a = \frac{P_3}{CL_{int} + P_3}\left\{1 - \exp\left(-\alpha_1 \times \frac{CL_{int} + P_3}{P_2}\right)\right\} \quad [60]$$

Here, the reduction of $P_2$ is directly reflected in the change in $F_a$ (fig. 24 right panel). This indicates that $F_a$ is increased with the reduction in $P_2$ when the initial value of $P_2$ is large, i.e., in the case of the drugs extensively transported out of the cell into the lumen. This effect of reducing $P_2$ is more marked if the influx clearance of the drug into the cell ($\alpha_1$) is relatively small (fig. 24 right panel). The results in figure 24 suggest that the effect of p-gp inhibition caused by drug-drug interactions on drug absorption may depend on the relative

extent of each process (influx from the lumen into the epithelial cell, efflux from the cell to the lumen, intracellular metabolism, and transport from the cell to the portal vein).

In the future, in addition to metabolic studies using human gut samples, drug-drug interactions involving the efflux process should be quantitatively evaluated by transport studies using intestinal brush border membrane vesicles to allow for more precise predictions of in vivo drug-drug interactions.

## REFERENCES


Aronoff GR, Bergstrom RF, Pottratz ST, Sloan RS, Wolen RL and Lemberger L (1984) Fluoxetine kinetics and protein binding in normal and impaired renal function. *Clin Pharmacol Ther* **36:**138–144.

Back DJ, Tjia JF, Karbwang J and Colbert J (1988) In vitro inhibition studies of tolbutamide hydroxylase activity of human liver microsomes by azoles, sulfonamides and quinolines. *Br J Clin Pharmacol* **26:**23–29.

Benet LZ (1995) Interspecies scaling: New lessons utilizing metabolic isozymes and pharmacokinetics, in *International Symposium on Strategy of Drug Metabolism Study for New Drug Development, Tokyo, Japan, June 13–15.* pp 43–46.

Benet LZ (1996) Problems and progress: From Bio-International '89 to the present, in *FIP Bio-International '96, Tokyo, Japan, April 22–24.* pp 9–13.

Bergstrom RF, Peyton AL and Lemberger L (1992) Quantification and mechanism of the fluoxetine and tricyclic antidepressant interaction. *Clin Pharmacol Ther* **51:** 239–248.

Bertz RJ and Granneman GR (1997) Use of in vitro and in vivo data to estimate the likelihood of metabolic pharmacokinetic interactions. *Clin Pharmacokinet* **32:**210–258.

Chiba M, Nishime JA and Lin JH (1995) Potent and selective inactivation of human liver microsomal cytochrome P-450 isoforms by L-754,394, an investigational human immune deficiency virus protease inhibitor. *J Pharmacol Exp Ther* **275:** 1527–1534.

Christensen LK, Hansen JM and Kristensen M (1963) Sulphaphenazole-induced hypoglycaemic attacks in tolbutamide-treated diabetics. *Lancet* **2:**1298–1301.

Daneshmend TK, Warnock DW, Ene MD, Johnson EM, Potten MR, Richardson MD and Williamson PJ (1984) Influence of food on the pharmacokinetics of ketoconazole. *Antimicrob Agents Chemother* **25:**1–3.

Daneshmend TK, Warnock DW, Turner A and Roberts CJC (1981) Pharmacokinetics of ketoconazole in normal subjects. *J Antimicrob Chemother* **8:**299–304.

Desgranges C, Razaka G, De Clercq E, Herdewijn P, Balzarini J, Drouillet F and Bricaud H (1986) Effect of (E)-5-(2-Bromovinyl)uracil on the catabolism and antitumor activity of 5-fluorouracil in rats and leukemic mice. *Cancer Res* **46:**1094–1101.

de Waziers I, Cugnenc PH, Yang CS, Leroux J-P and Beaune PH (1990) Cytochrome P450 isoenzymes, epoxide hydrolase and glutathione transferases in rat and human hepatic and extrahepatic tissues. *J Pharmacol Exp Ther* **253:**387–394.

Garteiz DA, Hook RH, Walker BJ and Okerholm RA (1982) Pharmacokinetics and biotransformation studies of terfenadine in man. *Arzneim-Forsch* **32:**1185–1190.

Gomez DY, Wacher VJ, Tomlanovich SJ, Hebert MF and Benet LZ (1995) The effects of ketoconazole on the intestinal metabolism and bioavailability of cyclosporine. *Clin Pharmacol Ther* **58:**15–19.

Guay DRP, Awni WM, Peterson PK, Obaid S, Breitenbucher R and Matzke GR (1987) Pharmacokinetics of ciprofloxacin in acutely ill and convalescent elderly patients. *Am J Med* **82:**124–129.

Gupta SK, Bakran A, Johnson RWG and Rowland M (1989) Cyclosporin-erythromycin interaction in renal transplant patients. *Br J Clin Pharmacol* **27:** 475–481.

Hebert MF, Roberts JP, Prueksaritanont T and Benet LZ (1992) Bioavailability of cyclosporine with concomitant rifampin administration is markedly less than predicted by hepatic enzyme induction. *Clin Pharmacol Ther* **52:**453–457.

Honig PK, Woosley RL, Zamani K, Conner DP and Cantilena LR Jr (1992) Changes in the pharmacokinetics and electrocardiographic pharmacodynamics of terfenadine with concomitant administration of erythromycin. *Clin Pharmacol Ther* **52:** 231–238.

Honig PK, Wortham DC, Zamani K, Conner DP, Mullin JC and Cantilena LR (1993) Terfenadine-ketoconazole interaction. *JAMA* **269:**1513–1518.

Hori R, Takano M, Okano T, Kitazawa S and Inui K (1982) Mechanisms of p-aminohippurate transport by brush-border and basolateral membrane vesicles isolated from rat kidney cortex. *Biochim Biophys Acta* **692:**97–100.

Hunter WC (1951) Oral administration of procaine penicillin with and without benemid p-(di-n-propylsulphanyl) benzoic acid. *Lancet* **261:**105.

Ito K, Iwatsubo T, Kanamitsu S, Nakajima Y and Sugiyama Y (1998) Quantitative prediction of in vivo drug clearance and drug interactions from in vitro data on metabolism together with binding and transport. *Annu Rev Pharmacol Toxicol,* **38:**461–499.

Iwatsubo T, Hirota N, Ooie T, Suzuki H, Shimada N, Chiba K, Ishizaki T, Green CE, Tyson CA and Sugiyama Y (1997) Prediction of in vivo drug metabolism in the human liver from in vitro metabolism data. *Pharmacol Ther* **73:**147–171.

Iwatsubo T, Hirota N, Ooie T, Suzuki H and Sugiyama Y (1996) Prediction of in vivo drug disposition from in vitro data based on physiological pharmacokinetics. *Biopharm Drug Dispos* **17:**273–310.

Jurima-Romet M, Crawford K, Cyr T and Inaba T (1994) Terfenadine metabolism in human liver: In vitro inhibition by macrolide antibiotics and azole antifungals. *Drug Metab Dispos* **22:**849–857.

Jurima-Romet M, Huang HS, Beck DJ and Li AP (1996) Evaluation of drug interactions in intact hepatocytes: Inhibitors of terfenadine metabolism. *Toxicol In Vitro* **10:**655–663.

Kalow W and Tang BK (1991) Use of caffeine metabolite ratios to explore CYP1A2 and xanthine oxidase activities. *Clin Pharmacol Ther* **50:**508–519.

Knodell RG, Browne DG, Gwozdz GP, Brian WR and Guengerich FP (1991) Differential inhibition of individual human liver cytochromes P-450 by cimetidine. *Gastroenterology* **101:**1680–1691.

Kolars JC, Awni WM, Merion RM and Watkins PB (1991) First-pass metabolism of cyclosporin by the gut. *Lancet* **338:**1488–1490.

Kolars JC, Schmiedlin-Ren P, Schuetz JD, Fang C and Watkins PB (1992) Identification of rifampin-inducible P450IIIA4 (CYP3A4) in human small bowel enterocytes. *J Clin Invest* **90:**1871–1878.

Kunze KL and Trager WF (1993) Isoform-selective mechanism-based inhibition of human cytochrome P450 1A2 by furafylline. *Chem Res Toxicol* **6:**649–656.

Kusuhara H, Suzuki H and Sugiyama Y (1998) The role of p-glycoprotein and canalicular multispecific organic anion transporter (cMOAT) in the hepatobiliary excretion of drugs. *J Pharm Sci,* in press.

Lensmeyer GL, Wiebe DA and Carlson IH (1988) Deposition of nine metabolites of cyclosporine in human tissues, bile, urine, and whole blood. *Transplant Proc* **20:**614–622.

Li AP and Jurima-Romet M (1997) Applications of primary human hepatocytes in the evaluation of pharmacokinetic drug-drug interactions: Evaluation of model drugs terfenadine and rifampin. *Cell Biol Toxicol* **13:**365–374.

Miller LG, Prichrd JG, White CA, Vytla B, Feldman S and Bowman RC (1990) Effect of concurrent sucralfate administration on the absorption of erythromycin. *J Clin Pharmacol* **30:**39–44.

Miners JO, Smith KJ, Robson RA, McManus ME, Veronese ME and Birkett DJ (1988) Tolbutamide hydroxylation by human liver microsomes. *Biochem Pharmacol* **37:**1137–1144.

Monahan BP, Ferguson CL, Killeavy ES, Lloyd BK, Troy J and Cantilena LR (1990) Torsades de pointes occurring in association with terfenadine use. *JAMA* **264:** 2788–2790.

Murray M and Reidy GF (1990) Selectivity in the inhibition of mammalian cytochromes P-450 by chemical agents. *Pharmacol Rev* **42:**85–101.

Nakamura H, Sano H, Yamazaki M and Sugiyama Y (1994) Carrier-mediated active transport of histamine $H_2$ receptor antagonists, cimetidine and nizatidine, into isolated rat hepatocytes: Contribution of Type 1 system. *J Pharmacol Exp Ther* **269:**1220–1227.

Nelson E and O'Reilly I (1961) Kinetics of carboxytolbutamide excretion following tolbutamide and carboxytolbutamide administration. *J Pharmacol Exp Ther* **132:** 103–109.

Oberle RL, Chen T-S, Lloyd C, Barnett JL, Owyang C, Meyer J and Amidon GL (1990) The influence of the interdigestive migrating myoelectric complex on the gastric emptying of liquids. *Gastroenterology* **99:**1275–1282.

Okuda H, Nishiyama T, Ogura K, Nagayama S, Ikeda K, Yamaguchi S, Nakamura Y, Kawaguchi Y and Watabe T (1995) Mechanism of lethal toxicity exerted by simultaneous administration of the new antiviral, sorivudine, and the antitumor agent, Tegafur. *Xenobio Metabol Dispos* **10**(Suppl)**:**166–169.

Okuda H, Nishiyama T, Ogura K, Nagayama S, Ikeda K, Yamaguchi S, Nakamura Y, Kawaguchi Y and Watabe T (1997) Lethal drug interactions of sorivudine, a new antiviral drug, with oral 5-fluorouracil prodrugs. *Drug Metab Dispos* **25:**270–273.

Parkinson A (1996) Biotransformation of xenobiotics, in *Casarett & Doull's Toxicology: The Basic Science of Poisons* (Klaassen CD ed) ed 5, pp 113–186, McGraw-Hill, New York.

Periti P, Mazzei T, Mini E and Novelli A (1992) Pharmacokinetic drug interactions of macrolides. *Clin Pharmacokinet* **23:**106–131.

Pharmaceutical Affairs Bureau, Japanese Ministry of Health and Welfare (1994) A report on investigation of side effects of sorivudine: Deaths caused by interactions between sorivudine and 5-FU prodrugs (in Japanese). June, 1994.

Pichard L, Fabre I, Fabre G, Domergue J, Saint Aubert B, Mourad G and Maurel P (1990) Cyclosporin A drug interactions: Screening for inducers and inhibitors of cytochrome P-450 (cyclosporin A oxidase) in primary cultures of human hepatocytes and in liver microsomes. *Drug Metab Dispos* **18:**595–605.

Preskorn SH, Beber JH, Faul JC and Hirschfeld RMA (1990) Serious adverse effects of combining fluoxetine and tricyclic antidepressants [letter]. *Am J Psychiatry* **147:**532.

Rolan PE (1994) Plasma protein binding displacement interactions—why are they still regarded as clinically important? *Br J Clin Pharmacol* **37:**125–128.

Rowland M and Martin SB (1973) Kinetics of drug-drug interactions. *J Pharmacokinet Biopharm* **1:**553–567.

Rowland M and Tozer TN (1995) Interacting drugs, in *Clinical Pharmacokinetics: Concepts and Applications* (Rowland M and Tozer TN eds) pp 267–289, Williams & Wilkins, Philadelphia.

Saitoh H and Aungst BJ (1995) Possible involvement of multiple P-glycoprotein-mediated efflux systems in the transport of verapamil and other organic cations across rat intestine. *Pharmaceut Res* **12:**1304–1310.

Sasabe H, Terasaki T, Tsuji A and Sugiyama Y (1997) Carrier-mediated hepatic uptake of quinolone antibiotics in the rat. *J Pharmacol Exp Ther* **282:**162–171.

Sathirakul K, Suzuki H, Yamada T, Hanano M and Sugiyama Y (1994) Multiple transport systems for organic anions across the bile canalicular membrane. *J Pharmacol Exp Ther* **268:**65–73.

Schellens JHM, Ghabrial H, van der Wart HHF, Bakker EN, Wilkinson GR and Breimer DD (1991) Differential effects of quinidine on the disposition of nifedipine, sparteine, and mephenytoin in humans. *Clin Pharmacol Ther* **50:**520–528.

Schuetz EG, Beck WT and Schuetz JD (1996) Modulators and substrates of P-glycoprotein and cytochrome P4503A coordinately up-regulate these proteins in human colon carcinoma cells. *Mol Pharmacol* **49:**311–318.

Shimamura H, Suzuki H, Hanano M, Suzuki A, Tagaya O, Horie T and Sugiyama Y

(1994) Multiple systems for the biliary excretion of organic anions in rats: Liquiritigenin conjugates as model compounds. *J Pharmacol Exp Ther* **271:**370–378.
Shimamura H, Suzuki H, Tagaya O, Horie T and Sugiyama Y (1996) Biliary excretion of glucyrrhizin in rats: Kinetic basis for multiplicity in bile canalicular transport of organic anions. *Pharmaceut Res* **13:**1833–1837.
Silverman RB (1988) Mechanism-based enzyme inactivation, in *Chemistry and Enzymology,* vol 1, pp 3–30, CRC Press, Boca Raton.
Skjelbo E and Brosen K (1992) Inhibitors of imipramine metabolism by human liver microsomes. *Br J Clin Pharmacol* **34:**256–261.
Slater LM, Sweet P, Stupeckey M and Gupta S (1986) Cyclosporin A reverses vincristine and daunorubicin resistance in acute lymphatic leukemia in vitro. *J Clin Invest* **77:**1405–1408.
Somogyi A and Muirhead M (1987) Pharmacokinetic interactions of cimetidine 1987. *Clin Pharmacokinet* **12:**321–366.
Statkevich P, Fournier DJ and Sweeney KR (1993) Characterization of methotrexate elimination and interaction with indomethacin and flurbiprofen in the isolated perfused rat kidney. *J Pharmacol Exp Ther* **265:**1118–1124.
Stille W, Harder S, Mieke S, Beer C, Shah PM, Frech K and Staib AH (1987) Decrease of caffeine elimination in man during co-administration of 4-quinolones. *J Antimicrob Chemother* **20:**729–734.
Sugita O, Sawada Y, Sugiyama Y, Iga T and Hanano M (1981) Prediction of drug-drug interaction from in vitro plasma protein binding and metabolism. *Biochem Pharmacol* **30:**3347–3354.
Sugita O, Sawada Y, Sugiyama Y, Iga T and Hanano M (1984) Kinetic analysis of tolbutamide-sulfonamide interaction in rabbits based on clearance concept: Prediction of species difference from in vitro plasma protein binding and metabolism. *Drug Metab Dispos* **12:**131–138.
Sugiyama Y and Iwatsubo T (1996) Alteration of pharmacokinetic features caused by drug interactions. *Xenobio Metabol Dispos* **11:**286–293.
Sugiyama Y, Iwatsubo T, Ueda K and Ito K (1996) Strategic proposals for avoiding toxic interactions with drugs for clinical use during development and after marketing of a new drug pharmacokinetic consideration. *J Toxicol Sci* **21:**309–316.
Sugiyama Y and Ooie T (1993) Prediction of pharmacokinetics based on in vitro data, in *Methods and Techniques for Pharmacokinetic Studies* (Sugiyama Y ed) pp 87–108, Japanese Society for the Study of Xenobiotics, Tokyo.
Takano M, Inui K, Okano T, Saitoh H and Hori R (1984) Carrier-mediated transport systems of tetraethylammonium in rat brush-border and basolateral membrane vesicles. *Biochim Biophys Acta* **773:**113–124.
Tanigawara Y, Okumura N, Hirai M, Yasuhara M, Ueda K, Kioka N, Komano T and Hori R (1992) Transport of digoxin by human p-glycoprotein expressed in a porcine kidney epithelial cell line (LLC-PK1). *J Pharmacol Exp Ther* **263:**840–845.
Terao T, Hisanaga E, Sai Y, Tamai I and Tsuji A (1996) Active secretion of drugs from the small intestinal epithelium in rats by P-glycoprotein functioning as an absorption barrier. *J Pharm Pharmacol* **48:**1083–1089.
Thomas RC and Ikeda GJ (1966) The metabolic fate of tolbutamide in man and in the rat. *J Med Chem* **9:**507–510.
Thummel KE, O'Shea D, Paine MF, Shen DD, Kunze KL, Perkins JD and Wilkinson GR (1996) Oral first-pass elimination of midazolam involves both gastrointestinal and hepatic CYP3A-mediated metabolism. *Clin Pharmacol Ther* **59:**491–502.
Todhunter JA (1979) Reversible enzyme inhibition, in *Methods in Enzymology* (Purich DL ed) vol 63, pp 383–411, Academic Press, London.
Transon C, Leemann T and Dayer P (1996) In vitro comparative inhibition profiles of major human drug metabolising cytochrome P450 isozymes (CYP2C9, CYP2D6 and CYP3A4) by HMG-CoA reductase inhibitors. *Eur J Clin Pharmacol* **50:**209–215.
Tsuruo T, Iida H, Tsukagoshi S and Sakurai Y (1981) Overcoming of vincristine resistance in P388 leukemia, in vivo and in vitro through enhanced cytotoxicity of vincristine and vinblastine by verapamil. *Cancer Res* **41:**1967–1972.
Tucker GT (1992) The rational selection of drug interaction studies: Implications of recent advances in drug metabolism. *Int J Clin Pharmacol Ther Toxicol* **30:**550–553.
Vereerstraeten P, Thiry P, Kinnaert P and Toussaint C (1987) Influence of erythromycin on cyclosporine pharmacokinetics. *Transplantation* **44:**155–156.
Veronese ME, Miners JO, Randles D, Gregov D and Birkett DJ (1990) Validation of the tolbutamide metabolic ratio for population screening with use of sulfaphenazole to produce model phenotypic poor metabolizers. *Clin Pharmacol Ther* **47:**403–411.
von Moltke LL, Greenblatt DJ, Duan SX, Harmatz JS and Shader RI (1994) In vitro prediction of the terfenadine-ketoconazole pharmacokinetic interaction. *J Clin Pharmacol* **34:**1222–1227.
von Moltke LL, Greenblatt DJ, Harmatz JS, Duan SX, Harrel LM, Cotreau-Bibbo MM, Pritchard GA, Wright CE and Shader RI (1996) Triazolam biotransformation by human liver microsomes *in vitro:* Effects of metabolic inhibitors and clinical confirmation of a predicted interaction with ketoconazole. *J Pharmacol Exp Ther* **276:**370–379.
Wacher VJ, Wu C-Y and Benet LZ (1995) Overlapping substrate specificities and tissue distribution of cytochrome P450 3A and P-glycoprotein: Implications for drug delivery and activity in cancer chemotherapy. *Mol Carcinog* **13:**129–134.
Wagner F, Kalusche D, Trenk D, Jahnchen E and Roskamm H (1987) Drug interaction between propafenone and metoprolol. *Br J Clin Pharmacol* **24:**213–220.
Waley SG (1985) Kinetics of suicide substrates: Practical procedures for determining parameters. *Biochem J* **227:**843–849.
Watabe T (1996) Strategic proposals for predicting drug-drug interactions during new drug development: Based on sixteen deaths caused by interactions of the new antiviral sorivudine with 5-fluorouracil prodrugs. *J Toxicol Sci* **21:**299–300.
Wilkinson GR (1983) Plasma and tissue binding considerations in drug disposition. *Drug Metab Rev* **14:**427–465.
Wu C-Y, Benet LZ, Hebert MF, Gupta SK, Rowland M, Gomez DY and Wacher VJ (1995) Differentiation of absorption and first-pass gut and hepatic metabolism in humans: Studies with cyclosporine. *Clin Pharmacol Ther* **58:**492–497.
Yamada T, Niinuma K, Lemaire M, Terasaki T and Sugiyama Y (1997) Carrier-mediated hepatic uptake of the cationic cyclopeptide, octreotide, in rats: Comparison between in vivo and in vitro. *Drug Metab Dispos* **25:**536–543.
Yamazaki M, Nishigaki R, Suzuki H and Sugiyama Y (1995) Kinetic analysis of hepatobiliary transport of drugs: Importance of carrier-mediated transport. *Yakugaku Zasshi* **115:**953–977.
Yamazaki M, Suzuki H, Hanano M, Tokui T, Komai T and Sugiyama Y (1993) $Na^+$-independent multispecific anion transporter mediates active transport of pravastatin into rat liver. *Am J Physiol* **264:**G36–G44.
Yamazaki M, Suzuki H and Sugiyama Y (1996) Recent advances in carrier-mediated hepatic uptake and biliary excretion of xenobiotics. *Pharmaceut Res* **13:**497–513.
Zomorodi K and Houston JB (1995) Effect of omeprazole on diazepam disposition in the rat: In vitro and in vivo studies. *Pharmaceut Res* **12:**1642–1646.